SUB-DIVIDING BROCA'S REGION BASED ON FUNCTIONAL CONNECTIVITY: NEW METHODS FOR INDIVIDUAL-LEVEL IN VIVO CORTICAL PARCELLATION

Der Fakultät für Biowissenschaften, Pharmazie und Psychologie

der Universität Leipzig

genehmigte

D I S S E R T A T I O N

Zur Erlangung des akademischen grades

Doktor rerum naturalium

Dr. rer. Nat.

Vorgelegt

Von Estrid Nystrup Jakobsen, MSc

geboren am 04. Juni 1989 in Fredensborg, Dänemark

Dekan:	Prof. Dr. Erich Schröger
Gutachter:	Prof. Dr. Rudolf Rübsamen
	Prof. Dr. Michael Petrides
Tag der Verteidigung:	Leipzig, den 02.06.2017

Overall, the human brain is the most complex object known in the universe - known, that is, to itself.

- E. O. Wilson

Bibliographical data

Broca's region is a part of the inferior frontal cortex known to be involved in language processing and is comprised of two distinct cytoarchitectonic areas, 44 and 45. The work described in the the present thesis aims to make use of prior knowledge of the anatomical locations and connectivity differences within Broca's region to delineate the extent and boundaries of areas 44 and 45 in individual brains. The thesis is comprised of two main projects.

The first project presents an initial application of a novel functional connectivity visualization technique for the manual parcellation of cortical areas in individual brains. This technique makes use of connectivity priors in conjunction with morphological information to manually delineate the extent and boundaries of cortical areas in individual brains. Results are presented from the application of the technique to the subdivision of Broca's region into its constituent areas 44 and 45 in a large number of individuals. Group-level comparisons of the resulting manual labels are consistent with previous findings regarding the connectivity and morphology of areas 44 and 45, and the manually labeled datasets can therefore be considered as the current gold standard for targeted individual-level *in vivo* cortical parcellation.

The second project builds on the results of project 1 by developing an automated and data-driven cortical parcellation technique that mimics the manual labeling approach to produce area labels with comparable precision at the individual level. While the manual parcellation method provides a reliable way to define cortical regions, it is also highly labor- and time-intensive and relies heavily on the expertise of the user. For this reason, the development of an observer-independent alternative technique is an important step in the overall research agenda. The automated parcellation technique is again applied to the sub-parcellation of Broca's region into its constituent areas 44 and 45 in a large number of individual brains, and the results of the manual and automated labeling approaches are compared at the individual level.

The methods presented as part of the two main projects have a number of potential applications within both research and clinical contexts, which are discussed in the final chapter of the current thesis. Additionally, future research directions relevant to the two main projects are described.

Acknowledgements

First and foremost I would like to express my gratitude to my supervisor, Dr. Daniel Margulies, for the continued support and supervision throughout my PhD studies. Your patience, encouragement, and belief in me through the times that I needed it most has been invaluable. The dedication you show to your work is truly inspiring and it has been an immense pleasure to work with you.

I would also like to thank Prof. Dr. Rudolf Rübsamen for agreeing to co-supervise my thesis. Your helpful advice, critical comments, and words of encouragement have been very valuable to me.

Additionally, I would like to thank Prof. Dr. Robert Turner and PD Dr. Stefan Geyer for providing me with the facilities and financial support to acquire dedicated computational resources necessary to conduct this research.

I am also grateful to Prof. Dr. Michael Petrides and Prof. Dr. Pierre Bellec for their insightful comments and fruitful collaborations, and for introducing me to the beautiful city of Montreal, where I will start the next chapter of my research career.

I am thankful to the International Max Planck Research School for the Neuroscience of Communication (IMPRS NeuroCom) for their financial support of the first three years of my PhD, and the FAZIT-Stiftung for awarding me with an 8-month completion grant, which has supported me during the last months of my PhD research.

I thank my colleagues of the Max Planck Research Group for Neuroanatomy and Connectivity for the stimulating discussions and for all the fun we have had over the years.

Last but not the least, I would like to thank all of my closest friends and family, without whom the last few years would have been a lot more difficult and a lot less fun. Words cannot express how grateful I am to have so many wonderful people in my life.

Table of contents

Abbreviations

aalf: anterior ascending ramus of the lateral fissure
AnG: angular gyrus
a: anterior
aSmG: anterior supramarginal gyrus
BA: Brodmann area
BOLD: blood-oxygenation-level dependent
cgs: cingulate sulcus
cs: central sulcus
d: dorsal
DC: dorsocaudal
dMRI: diffusion-weighted magnetic resonance imaging
ds: diagonal sulcus
fMRI: functional magnetic resonance imaging
half: horizontal anterior ramus of the lateral fissure
HCP: Human Connectome Project
ICA: independent component analysis
ifs: inferior frontal sulcus
iprs: inferior precentral sulcus
lf: lateral fissure
MRI: magnetic resonance imaging
NKI: enhanced Nathan Kline Institute - Rockland Sample
Op: pars opercularis
p: posterior
PF: area PF
PFG: area PFG
PG: area PG
PGm: central precuneal region
PMCm: middle posteromedial cortex
Pre-SMA: pre-supplementary motor area
ProM: proisocortical motor area
pSmG: posterior supramarginal gyrus
R: rostral
ROI: region of interest
rs-fMRI: resting-state functional magnetic resonance imaging
SMA: supplementary motor area
STS: superior temporal sulcus
STSa: anterior superior temporal sulcus
STSm: middle superior temporal sulcus
STSp: posterior superior temporal sulcus
Tr: pars triangularis
ts: triangular sulcus
v: ventral
VC: ventrocaudal
VR: ventrorostral
44: area 44
45: area 45
6VR: ventrorostral area 6

Chapter 1 - Introduction to topic and methods

1.1 Broca's region

1.1.1 History and discovery

One of the fundamental guiding principles of human cognitive neuroscience is the idea that the cerebral cortex can be subdivided into a number of distinct regions that serve different cognitive functions. This idea of functional modularity originates from the 19th century movement known as phrenology, led by Franz Joseph Gall and Johann Gaspar Spurzheim. According to the theory of phrenology, aspects of a person's intellectual faculties and personality could be determined by the size and shape of bumps on the skull (Figure 1.1; Gall and Spurzheim 1818). Although phrenology has long since been disregarded as pseudoscience, later historical lesion case studies provided evidence for the concept of functional modularity of the brain, which now serves as a cornerstone of modern neuroscience.
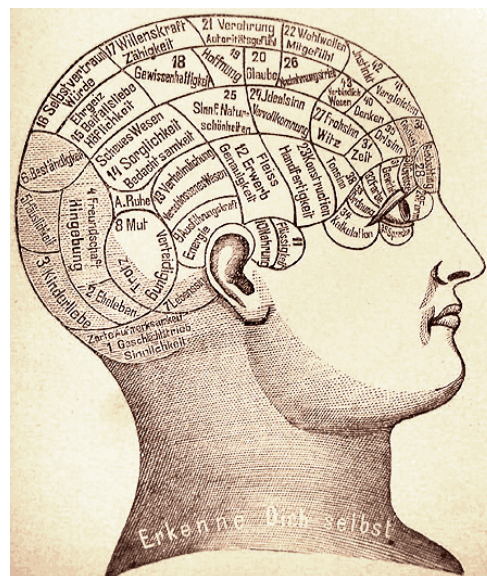
Figure 1.1: A phrenological map of the human cranium. It was believed that the shape and size of bumps on the skull determine aspects of a person's personality and intellectual faculties. (image from Bilz 1894 via Wikimedia Commons)

Perhaps the most well-known examples of historical lesion case studies are those by French physician Pierre Paul Broca (Broca 1861a, b, and c). In 1861, Broca encountered a 51-year-old male patient named Leborgne who was unable to speak any words other than "tan", but was otherwise unimpaired. After Leborgne's death, an autopsy revealed a lesion in the frontal part of the left cerebral hemisphere, as predicted by lingering claims of phrenologists that language function originated in the left frontal lobe. A few months later, Broca encountered a second 84-year-old patient named Lelong, who presented with similar aphasic symptoms as the result of a stroke. Lelong's vocabulary was limited to only five simple words, some of which were mispronounced, including his own name. Once again, autopsy revealed severe damage to the same region of the lateral frontal lobe (Figure 1.2), which led to the conclusion that articulated language must be localized in the third convolution of the left inferior frontal gyrus.
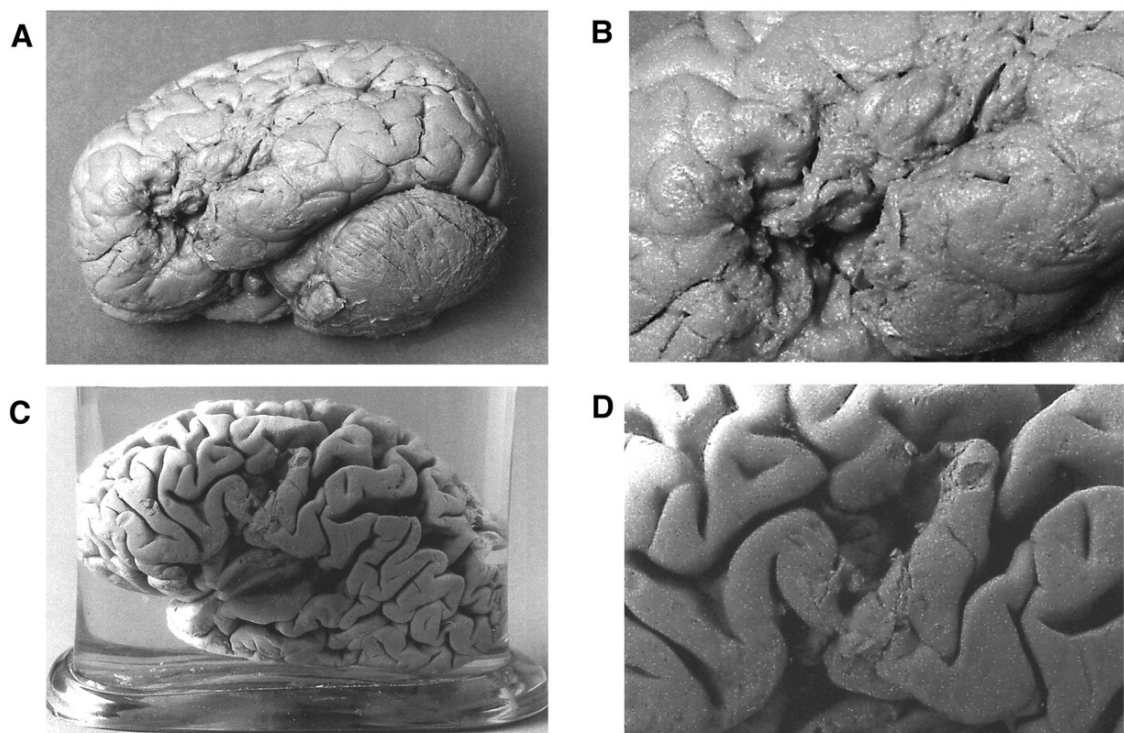
Figure 1.2: The brains of Broca's patients, Leborgne (A and B) and Lelong (C and D). Both patients' brains exhibited damage to the inferior frontal cortex. (image from Dronkers et al. 2007)

Within the following years, Broca collected a number of similar lesion cases to support his hypothesis, the careful documentation of which was central to establishing the role of the left inferior frontal gyrus in speech production. This region is now known as Broca's region and is one of the most widely studied brain areas due to its historical significance and established involvement in language processing.

1.1.2 Cytoarchitectonic differentiation and macroscopic landmarks

Traditionally, Broca's region refers to the posterior part of the inferior frontal gyrus, but it can be subdivided into two distinct cytoarchitectonic areas: Brodmann areas 44 and 45 (Figure 1.3). By staining the cell bodies of neurons and glial cells in tissue samples (known as Nissl staining), six layers of neurons in the cerebral cortex can be identified, which are referred to by roman numerals I-VI. Cytoarchitectonic differentiation refers to defining cortical areas and their boundaries based on differences in the cellular architecture of these cortical layers.

Area 44 is described as dysgranular due to its not fully developed cortical layer IV. This is the fundamental cytoarchitectonic feature that distinguishes it from its neighboring areas, including caudally adjacent premotor area 6, which is agranular due to an absence of layer IV, and rostrally adjacent area 45, in which layer IV is fully developed. Area 45 is described as granular cortex due to its well developed layer IV, containing small stellate neurons, which distinguishes it from neighboring area 44. Area 45 also contains many unusually large pyramidal cells, known as magnopyramidal neurons, in the deepest part of layer III, which distinguishes it from its surrounding prefrontal areas (Figure 1.3; Petrides and Pandya 2002). Due to the rostral-caudal progression from granular area 45 to dysgranular area 44 to agranular area 6, area 44 has been described a transitional area between the orofacial part of premotor area 6 and the ventral prefrontal cortex (Petrides 2013). It is also worth noting that area 45 can be further subdivided into cytoarchitectonic subregions 45A and 45B, based mainly on the relative development of layer IV (Gerbella 2010). However, since the studies presented in the current thesis do not

attempt to distinguish areas 45A and 45B, these two subregions will henceforth be referred to collectively as area 45.
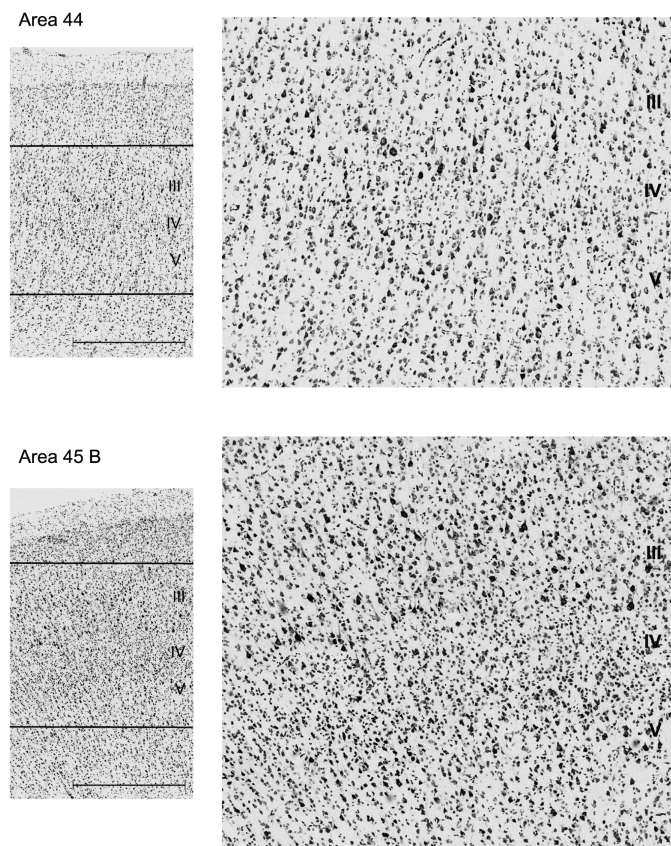
Figure 1.3: Photomicrographs showing the cytoarchitectonic structure of homologue areas 44 and 45 in the macaque monkey, defined by the same criteria as used to define these regions in the human brain. Note that layer IV is fully developed in area 45, but not in area 44. (Image from Petrides and Pandya 2009)

Macroscopically, area 44 is located on the pars opercularis, which is defined as the portion of the inferior frontal gyrus that lies ventral to the inferior frontal sulcus and anterior to the inferior precentral sulcus. Area 45 is located on the pars triangularis, which is located between the horizontal and anterior ascending rami of the lateral fissure on the inferior frontal gyrus, and is dorsally bounded by the inferior frontal sulcus. The macroscopic landmark separating areas 44 and 45 is therefore the anterior ascending ramus of the lateral fissure (Figure 1.4; Amunts et al. 1999, 2010; Petrides and pandya 1994, 2002). While the macroscopic definitions of cortical areas are based on the findings from cytoarchitectonic studies, it is important to note that individual-

level observer-independent delineation of the cytoarchitectonic borders of areas 44 and 45 did not reveal consistent correspondence with sulcal contours (Amunts et al. 1999).
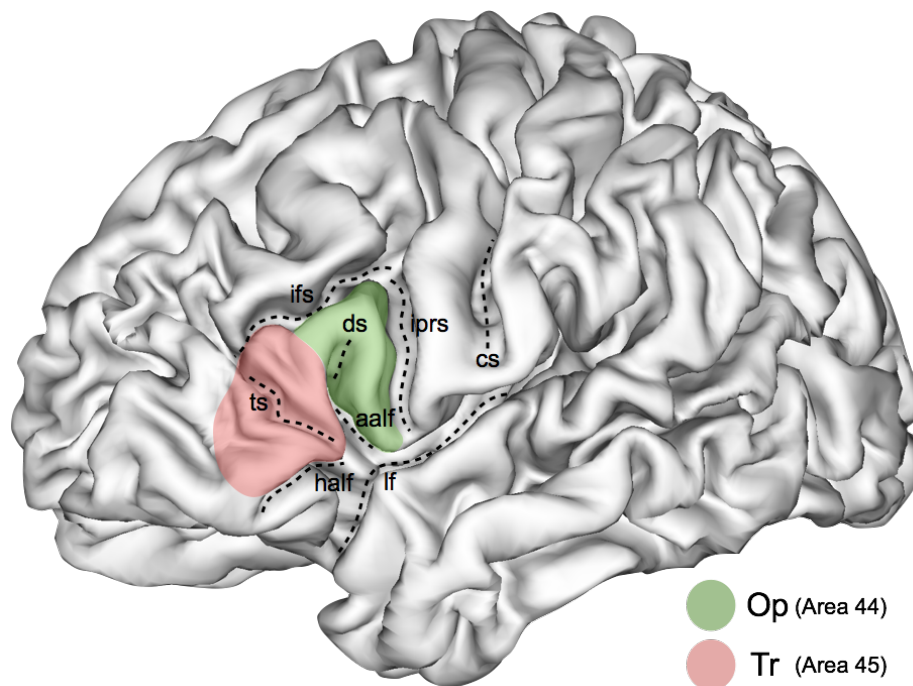
Figure 1.4: Macroscopic landmarks used to define areas 44 and 45 in individual brains based on cytoarchitectonic studies. aalf, anterior ascending ramus of the lateral fissure; cs, central sulcus; ds, diagonal sulcus; half, horizontal anterior ramus of the lateral fissure; ifs, inferior frontal sulcus; iprs, inferior precentral sulcus; lf, lateral fissure; Op, pars opercularis; Tr, pars triangularis; ts, triangular sulcus.

1.1.3 Functional dissociation

The cytoarchitectonic differentiation of areas 44 and 45 is corroborated by functional dissociation. Early direct cortical stimulation studies in humans by Penfield and Roberts (1959) provided the first evidence of functional differentiation between areas 44 and 45. Specifically, they showed that stimulation of area 6, which lies directly posterior to area 44, causes vocalization, while stimulation of area 44 and caudal area 45 leads to speech arrest (see also Rasmussen and Milner, 1975; Ojemann et al., 1989). Contrary to these results, a recent direct cortical stimulation study localized speech arrest to the ventral premotor cortex, and not area 44, while finding foci for anomia/paraphasia within the inferior and middle frontal gyri (Tate et al. 2014). Modern functional magnetic resonance imaging (fMRI) studies have also suggested a

functional specialization of areas 44 and 45. Though there is some discrepancy regarding the precise range of functions that can be attributed to these two areas, it is generally agreed that while area 44 is mainly involved in speech production, area 45 is more involved in higher-level semantic aspects of language processing such as verbal fluency (Amunts et al. 2004; Heim et al. 2005; Katzev et al. 2013) and controlled cognitive retrieval of verbal information (e.g. Petrides et al. 1995; Poldrack et al. 1999).

1.1.4 Connectivity differences

Based on findings from macaque monkey tract-tracing as well as diffusion-weighted magnetic resonance imaging (dMRI) studies, areas 44 and 45 are known to differ in their structural connectivity to superior temporal and inferior parietal regions in both macaque monkeys and humans (Figure 1.6; Petrides and Pandya 2002, 2009). The classical arcuate fasciculus links Broca's region with the superior temporal region and, in addition, provides an indirect connection via its local links with the inferior parietal region (Figure 1.5; Catani et al. 2005).
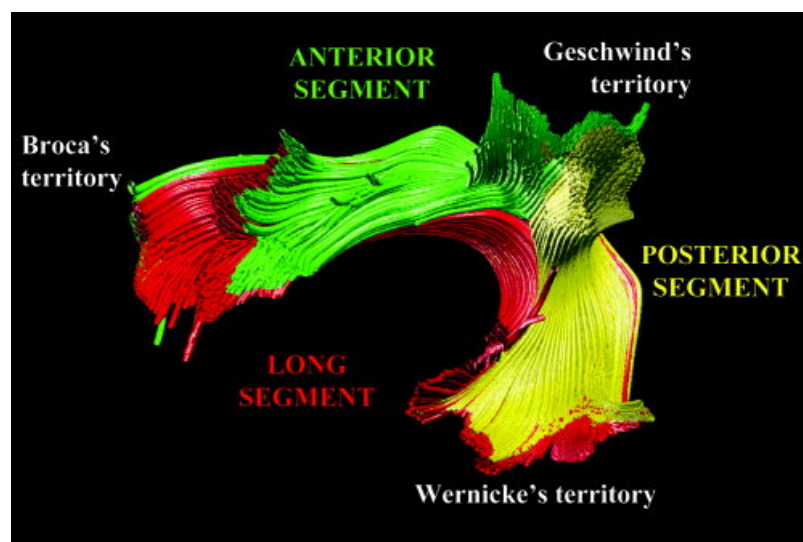
Figure 1.5: Tractography reconstruction of the arcuate fasciculus, which forms a core part of the classical Perisylvian language network. Broca's region is connected to Wernicke's territory in the temporal lobe via direct (red) and indirect (green and yellow) pathways. The indirect pathways additionally connect Geschwind's territory of the inferior parietal cortex. (Image from Catani et al. 2005)

This parietal region is in turn connected with ventrolateral frontal areas via the superior longitudinal fasciculus and to temporal areas via the extreme capsule fasciculus. More specifically, area 44 connects to the rostral inferior parietal lobule via the third branch of the superior longitudinal fasciculus, and area 45 connects to the superior temporal gyrus and superior temporal sulcus via the extreme capsule fasciculus (Anwander et al. 2007; Frey et al. 2008; Petrides and Pandya 2009).
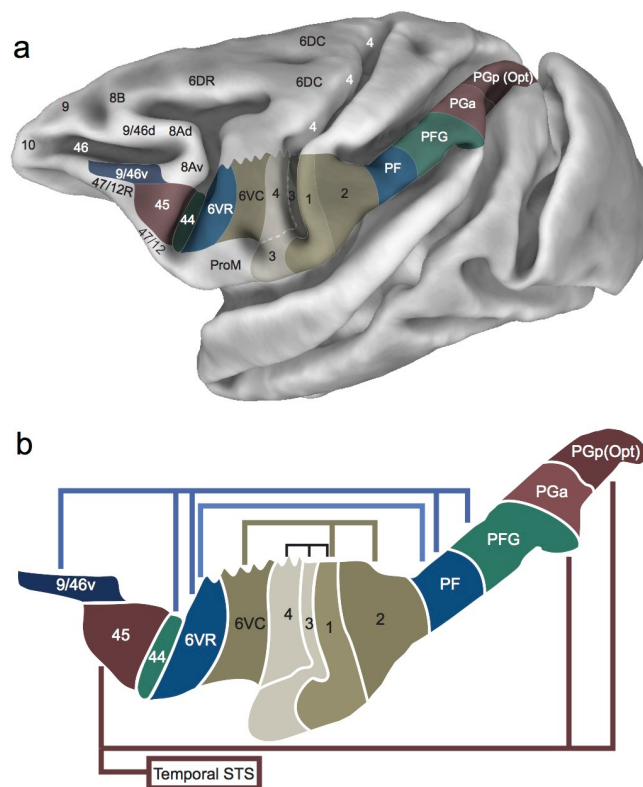
Figure 1.6: Schematic summary of the anatomical connectivity of ventrolateral frontal and inferior parietal cortex in the macaque monkey. Corresponding colors indicate connectivity between regions. Note the distinct connectivity of area 44 and 45 homologues. R, rostral; VR, ventrorostral; VC, ventrocaudal; DC, dorsocaudal; d, dorsal; v, ventral; a, anterior; p, posterior; STS, superior temporal sulcus; ProM, proisocortical motor area. (Image from Margulies and Petrides 2013)

A study by Kelly et al. (2010) used spectral clustering to investigate functional connectivity in the human brain using resting-state fMRI (rs-fMRI) and provided preliminary evidence that the distinct connectivity profiles of areas 44 and 45 are consistent between humans and macaques. However, specific differences proved difficult to distinguish using group-level analysis due to the

high degree of individual variability in the topography of cortical areas. Following on from this study, recent work by Margulies and Petrides (2013) was able to distinguish areas 44 and 45 from each other and neighboring regions using seed-based resting-state functional connectivity in individual brains. Consistent with known structural connectivity differences, the main distinguishing functional connectivity features were found in the superior temporal and inferior parietal regions. The study presented in Chapter 2 of this thesis builds on this work, and specific differences in functional connectivity between areas 44 and 45 are discussed in detail in section 2.2.4. Additionally, Figure 2.2 provides a schematic summary of the known differences in connectivity patterns of areas 44 and 45, as well as neighboring premotor area 6, in the human brain.

1.2 General methods

1.2.1 Cortical parcellation

Methods that aim to identify meaningful subdivisions or boundaries between cortical regions based on homogeneity within and differences between areas in their structure, function, and connectivity, can be collectively described as parcellation techniques. Perhaps the most well-known map of the human cerebral cortex is that produced by Korbinian Brodmann in 1909, who used a parcellation technique based on the cytoarchitectonic features (i.e. the size, shape, distribution, and other properties of cell bodies) of the cortical layers in postmortem brains to subdivide the human cerebral cortex into 52 distinct areas (Figure 1.7; Brodmann 1909). For historical reasons, Brodmann's schematic map of the human cerebral cortex is still widely used as a reference for the identification of cortical regions in the fields of human neuroimaging and cognitive neuroscience, but with the rapid development of high-resolution neuroimaging techniques, it is now possible to characterize brain areas *in vivo* based on macro-scale structural and functional properties. These developments represent a significant leap forward in

neuroscience and have opened the door for studying the relationship and correspondence between structure and function in the living human brain.
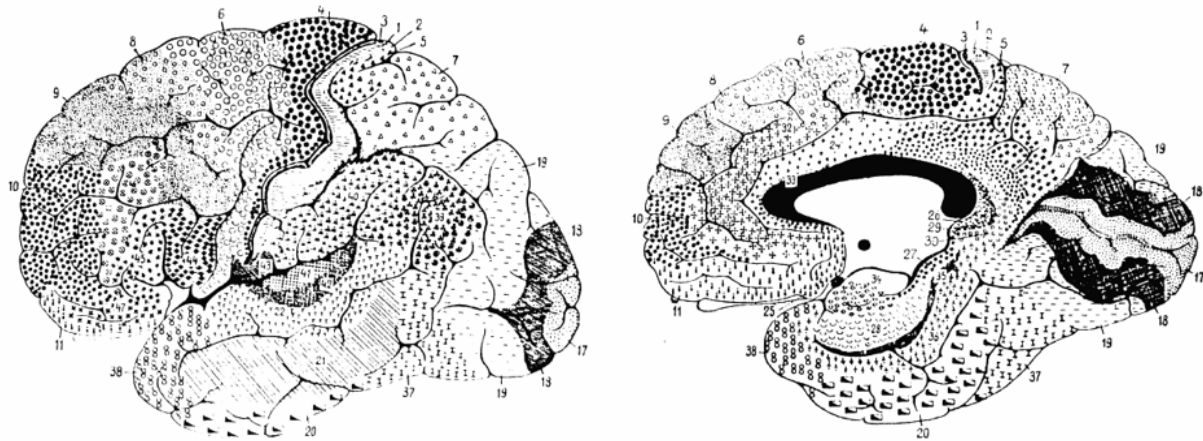
Figure 1.7: Brodmann's map of the human cerebral cortex. The cortex is divided into 52 distinct regions based on cytoarchitectonic features (image from Brodmann, Korbinian: Vergleichende Lokalisationslehre der Grosshirnrinde, 1909. via Wikimedia Commons)

1.2.2 Distributive processing and functional networks

In the context of cognitive neuroscience, the theory of distributive processing (Mesulam 1990) suggests that brain areas are highly interconnected and process information in a distributed manner. Although originally thought of as competing and contradictory theories of brain functioning, the concepts of functional modularity and distributed processing are not mutually exclusive, and provide the most intuitive explanation of brain functioning when combined to complement the concept of functional networks.

While the shift in neuroscientific research towards a network-based approach for understanding brain function is relatively recent, the notion of brain networks has been around much longer. Brodmann (1909) argued that the cytoarchitectonic boundaries he observed were functionally significant, and that each cortical area plays a role in a larger and more distributed functional network (Amunts and Zilles 2015). It is now widely agreed that brain-behavior relationships are

both localized, or modular, and distributed and that complex cognitive domains are likely to arise from interactions between multiple distributed brain regions with complex computational architectures. Such functional networks can be defined as either local, if they are confined to immediately neighboring areas or a single cytoarchitectonic region, or large-scale, if they are composed of several interconnected local networks (Mesulam 1990).

Due to the inevitable complexity of brain organization given this type of network structure, it is necessary extend the concept of a functional module to include information regarding its role and position within large-scale brain networks, rather than assigning it a single definitive function. Functional connectivity information therefore provides an appropriate basis upon which to define cortical regions.

1.2.3 Resting-state fMRI and functional connectivity

Functional magnetic resonance imaging (fMRI) is a neuroimaging method that uses local changes in blood flow as a proxy for brain activity. This technique relies on the so-called blood oxygenation-level dependent (BOLD) effect as the basis for image contrast (Ogawa 1990). When a specific brain region increases its activity in response to a stimulus, there is a corresponding increase in the amount of oxygen consumed in that region of the brain. Owing to the inherent differences in the paramagnetic properties of oxygenated and deoxygenated blood, fMRI allows us to detect these local changes and gain an approximate measure of neural activity in different brain regions over time.

While classical fMRI studies rely on task-induced BOLD responses (for example by localizing brain regions that increase activity during mental arithmetic), resting-state fMRI (rs-fMRI) instead measures the intrinsic spontaneous low-frequency fluctuations in BOLD activity occurring in the absence of explicit task performance or stimuli (Figure 1.8; Biswal 1995). By correlating the time-courses of these intrinsic fluctuations across different brain regions, we can

infer that regions whose activity fluctuate at the same or similar frequencies must be functionally connected, facilitating the study of brain organization via functional networks (Van Den Heuvel and Pol 2010). Using rs-fMRI, one can thereby derive the functional connectivity "fingerprints" characterizing different cortical regions serving different cognitive functions, and use this information as the basis for a variety of applications, including cortical parcellation.
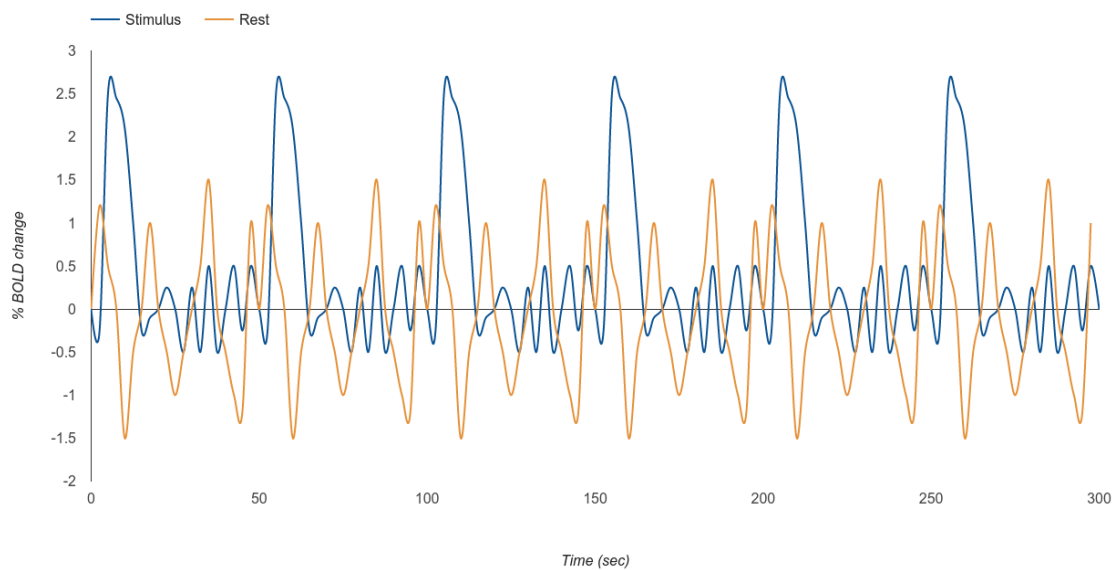
Figure 1.8: Theoretical data showing the percentage of BOLD change over time as measured by classical task-based (blue) and resting-state (orange) fMRI. Presentation of stimuli during a task induce spikes in BOLD response, while the resting state is characterized by spontaneous low-frequency BOLD fluctuations.

Although measures of functional and structural connectivity are fundamentally different due to the vastly different underlying measurements, there is evidence that functional connectivity derived from rs-fMRI reflects the underlying anatomy and provides meaningful insight to brain network organization (see Fox and Raichle 2007 for a review of this topic). This evidence comes largely through comparison to macaque monkey tract tracing studies, which allow for precise descriptions of neuronal projections by the direct injection of axonal tracer molecules into particular regions of the cortex (Vincent et al. 2007; Margulies et al. 2009; Mars et al. 2011; Hutchison and Everling 2012; Hutchison et al. 2013; Sallet et al. 2013). Additional support for the consistency between functional and structural connectivity in humans comes from diffusion-

weighted MRI studies. dMRI is able to provide an indirect measure of structural connectivity *in vivo*, by quantifying the diffusion of water molecules along the axons that make up white matter fiber bundles (Le Bihan et al. 1986). A review of eight studies that directly compared results from dMRI and rs-fMRI found an overall positive correlation between structural and functional connectivity strengths derived from the two imaging modalities (Damoiseaux and Greicius 2009). An advantage of rs-fMRI is that while dMRI is currently limited to resolving large-scale fiber bundles, rs-MRI is sensitive to both local and large-scale functional connectivity (Sepulcre et al. 2010). However, it is important to note that functional connectivity derived from rs-fMRI has been observed between regions that are not directly anatomically connected (Vincent et al. 2007; Honey et al. 2009; Miranda-Dominguez et al. 2014). It is likely that the presence of such functional connections is due to indirect structural connectivity (i.e. two regions are connected via a third region).

1.2.4 Visualization and exploration of high-dimensional data

The most basic way to represent functional connectivity information is as a two-dimensional matrix, where each point in the matrix represents the probability of connectivity (as measured by the correlation or similarity of the BOLD time-courses) between two points in the brain. With the advent of high-resolution neuroimaging techniques, such connectivity matrices often consist of hundreds of thousands of data points, requiring several gigabytes of computational memory, even without the addition of essential information regarding the anatomical location of each of those data points. This high dimensionality and resolution of functional connectivity data presents one of the biggest challenges of resting-state fMRI research, both in dealing with the sheer size of the datasets and in producing informative data visualizations.

For this reason, current functional connectivity visualization techniques rely on dramatically reducing the dimensionality of the data in order to make sense of it (see Margulies et al. 2013 for a review of connectivity visualization techniques). For example, a popular method for aiding

resting-state functional connectivity analyses is seed-based connectivity visualization. Using this technique, one can display the connectivity pattern of a user-defined region of interest (ROI) on the brain in order to observe the spatial organization of that region's connectivity profile. In its most interactive form, such as is implemented in the open-source software, brainGL (Böttger et al. 2014), the user simply clicks on any region on the cortical surface, and the corresponding row of the underlying correlation matrix is displayed on the cortical surface (Figure 1.9).
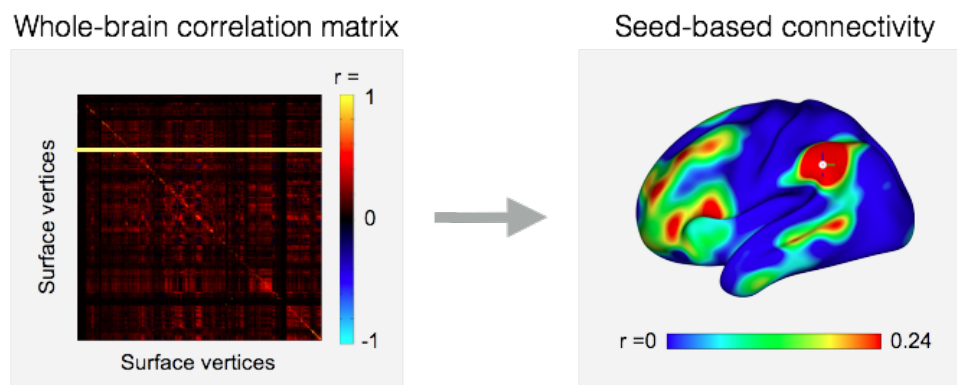
Figure 1.9: An illustration of seed-based functional connectivity analysis. An ROI, or seed, representing a vertex on the cortical surface is selected, and the corresponding connectivity vector is extracted from the whole-brain connectivity matrix and displayed on the cortical surface. The resulting map represents the strength of connectivity between the selected vertex and the rest of the cortical surface.

While this technique facilitates easy and interactive identification of distinct connectivity patterns of single regions of interest, it does not provide a method to map the extent and boundaries of the cortical areas that the chosen seed regions belong to, as this requires comparing the connectivity patterns of multiple neighboring seed regions simultaneously. This problem highlights the importance of the development of novel functional connectivity data visualization techniques designed to facilitate precise cortical parcellation. Additionally, seed-based connectivity analysis requires the investigator to pre-select an ROI, which could induce a selection bias. For this reason, the development of data-driven approaches for functional connectivity analysis is of high interest in the field of rs-fMRI research.

1.2.5 Data-driven cortical parcellation using resting-state fMRI

A different approach to dealing with the complexity of rs-fMRI data is to reduce its dimensionality by grouping data points that are similar into modules or networks to facilitate interpretation. Another focus of research within the field of rs-fMRI has therefore been on the development of data-driven cortical parcellation techniques based on functional connectivity (Thirion et al. 2014). These methods take as input either the timeseries of individual data points, or vertices on the cortex, or the corresponding connectivity vector, and subsequently make use of a various clustering algorithms to group data points according to the similarity of their connectivity patterns. This results in a set of non-overlapping regions or networks exhibiting homogeneity within and heterogeneity between their connectivity profiles (see for example Yeo and Krienen et al. 2011; Kahnt et al. 2012). While the resulting network maps have a variety of valuable applications such as serving as functional atlases of cortical regions, interpreting and evaluating their validity as definitive maps of the cerebral cortex is difficult. Most common clustering algorithms, such as k-means (Arthur and Vassilvitskii 2007) and hierarchical clustering (Murtagh and Legendre 2011), require the user to specify the number of clusters or networks the cortex should be divided into a priori. This is an implicit problem because there is no agreement upon how many regions or networks exist in the human brain, and it is possible that the number of networks may vary across individuals (Wang et al. 2015). One possible way to overcome this problem is to run the algorithm with a varying number of clusters and subsequently choose the solution that best reflects some pre-existing ontology of brain regions or anatomical atlas. Additionally, clustering techniques often treat neighboring vertices as entirely independent data points, which may not be appropriate when applied to brain organization, given that the voxel sampling resolution of rs-fMRI data may exceed the appropriate scale for defining regions based on their connectivity (Thirion et al. 2014).

In spite of the difficulties inherent in interpreting their results, data-driven parcellation methods are seen by many as favorable because they are, as the name suggests, driven by the data itself and therefore unbiased by the user. However, it is important to consider that by relying solely on the measured data, these methods fail to take advantage of the large amount of prior knowledge that exists about the morphology, variability, cytoarchitecture, and unique connectivity patterns of particular regions of the brain.

1.2.6 Individual variability and the importance of single-subject analysis

The study of individual differences in human brain anatomy has long been an established field of research. However, it is only recently that is has become possible to investigate functional differences *in vivo* using advanced neuroimaging techniques and thus examine the stability of relationships between structure and function across individuals. It is well-known that certain regions of the brain, especially those involved in higher-order cognitive functions, exhibit higher degrees of inter-subject morphological variability than primary sensory regions (Mueller et al. 2013; Gao et al. 2014), making it difficult to accurately distinguish areal boundaries within these regions based on macroanatomical landmarks alone. For this reason, it is necessary to develop tools for cortical parcellation at the individual level that allow us to procure subject-specific functional atlases.

1.2.7 Overview

The following chapters describe two main research projects, the overarching goal of which is to make use of prior knowledge of the anatomical locations and connectivity differences within Broca's region to delineate the extent and boundaries of areas 44 and 45 in individual brains. The first project, described in Chapter 2, makes use of a novel functional connectivity visualization technique to manually parcellate areas 44 and 45 in individual brains based on macroscopic landmarks and connectivity features. The resulting manual labels are compared at the group level and are shown to be highly consistent with previous findings relating to the

connectivity and morphology of areas 44 and 45. These manually labeled datasets can therefore be considered the current gold standard for individual-level *in vivo* cortical parcellation of areas 44 and 45. The second project, described in Chapter 3, builds on the results of the first project by developing an automated, observer-independent, and data-driven cortical parcellation technique that mimics the manual labeling approach. The main goal of this project is to automatically produce area labels with comparable precision to manual labeling at the individual level. The automated parcellation technique is again applied to the sub-parcellation of Broca's region into its constituent areas 44 and 45 in a large number of individual brains, and the results are compared to the gold standard manual labels at the individual level. The automated parcellation technique is applied to two independent datasets in order to demonstrate its ability to generalize to datasets with varying acquisition and preprocessing parameters. Finally, various applications and future directions relating to these two main projects are discussed in Chapter 4.

Chapter 2 - Subdivision of Broca's region based on individual-level functional connectivity

Abstract

Broca's region is composed of two adjacent cytoarchitectonic areas, 44 and 45, which have distinct connectivity to superior temporal and inferior parietal regions in both macaque monkeys and humans. The current study aimed to make use of prior knowledge of sulcal anatomy and resting-state functional connectivity, together with a novel visualization technique, to manually parcellate areas 44 and 45 in individual brains in vivo. One hundred and one resting-state functional magnetic resonance imaging datasets from the Human Connectome Project were used. Left-hemisphere surface-based correlation matrices were computed and visualized in brainGL. By observation of differences in the connectivity patterns of neighbouring nodes, areas 44 and 45 were manually parcellated in individual brains, and then compared at the group-level. Additionally, the manual labelling approach was compared with parcellation results based on several data-driven clustering techniques. Areas 44 and 45 could be clearly distinguished from each other in all individuals, and the manual segmentation method showed high test-retest reliability. Group-level probability maps of areas 44 and 45 showed spatial consistency across individuals, and corresponded well to cytoarchitectonic probability maps. Group-level connectivity maps were consistent with previous studies showing distinct connectivity patterns of areas 44 and 45. Data-driven parcellation techniques produced clusters with varying degrees of spatial overlap with the manual labels, indicating the need for further investigation and validation of machine learning cortical segmentation approaches. The current study provides a reliable method for individual-level cortical parcellation that could be applied to regions distinguishable by even the most subtle differences in patterns of functional connectivity.

2.1 Introduction

Broca's region is located on the inferior frontal gyrus in the language-dominant hemisphere, and forms a core part of the perisylvian language network. Cytoarchitectonic studies have differentiated two distinct areas within this region, areas 44 and 45, which are generally related to the gross morphological landmarks of the pars opercularis and triangularis, respectively (Figure 2.1) (Amunts et al., 1999).
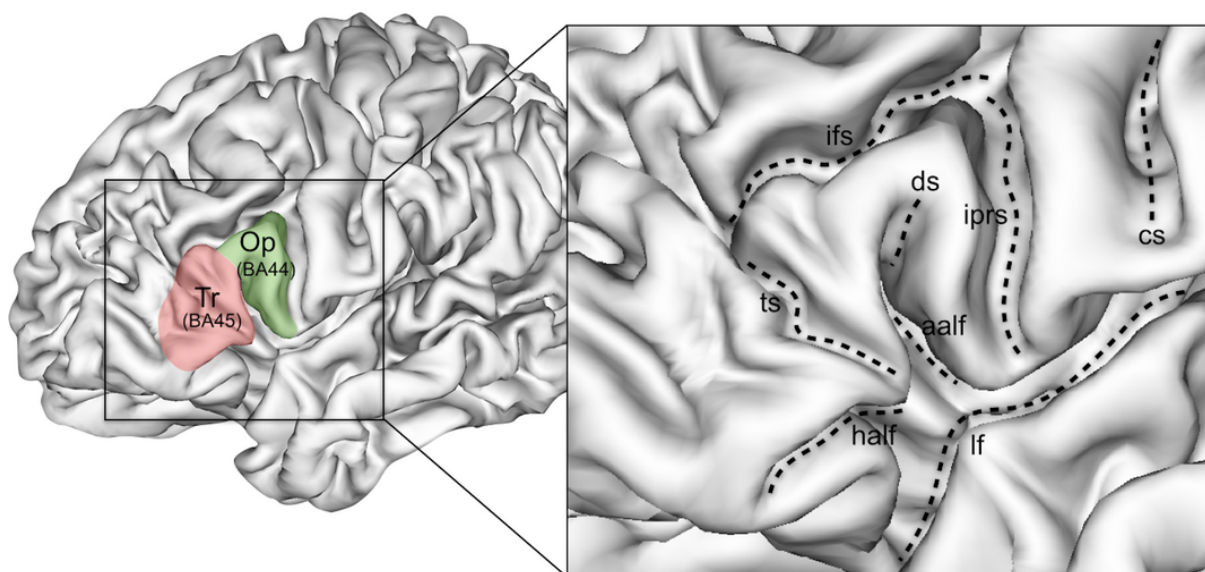
Figure 2.1. Anatomical landmarks of the inferior frontal gyrus in an individual subject. aalf, anterior ascending ramus of the lateral fissure; cs, central sulcus; ds, diagonal sulcus; half, horizontal anterior ramus of the lateral fissure; ifs, inferior frontal sulcus; iprs, inferior precentral sulcus; lf, lateral fissure; Op, pars opercularis; Tr, pars triangularis; ts, triangular sulcus.

Despite debates regarding the convergence of cytoarchitectonic borders with sulcal contours (Amunts et al., 1999), these anatomical criteria, derived from postmortem cytoarchitectonic data, are commonly used for the identification of areas 44 and 45 in *in vivo* magnetic resonance imaging (MRI) data (Fischl et al., 2002). Nonetheless, morphological studies have demonstrated that this part of the ventrolateral frontal cortex shows a high degree of individual variability in sulcal and gyral morphology (Keller et al., 2007), with some individuals entirely lacking either the horizontal or the anterior ascending ramus of the lateral fissure (Ono et al., 1990; Tomaiuolo et

al., 1999). For this reason, individual-level analysis and the integration of multimodal data are crucial for accurate delineation of these subdivisions within Broca's region.
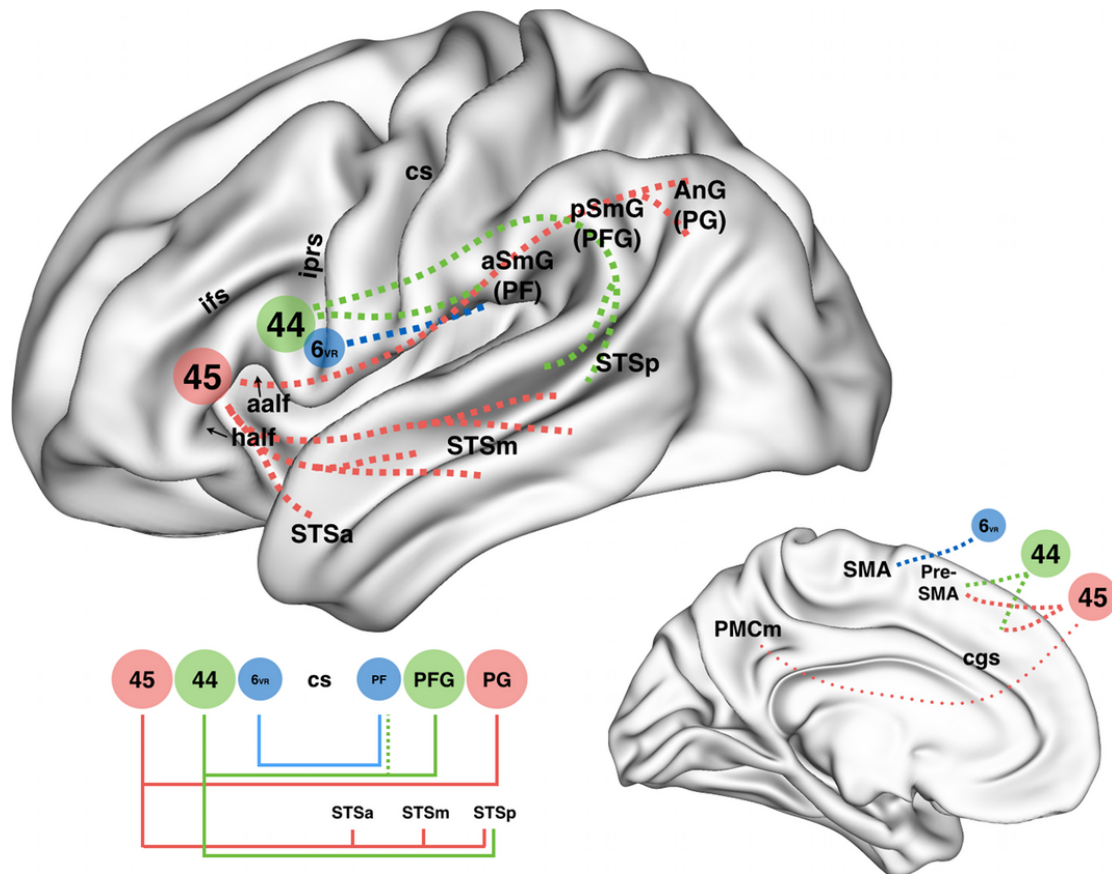
Figure 2.2. Schematic representation of the distinct connectivity profiles of areas 45 and 44, and the neighboring area 6VR (Petrides & Pandya, 2009; Kelly et al., 2010; Margulies & Petrides, 2013). aalf, anterior ascending ramus of the lateral fissure; AnG, angular gyrus; aSmG, anterior supramarginal gyrus; cgs, cingulate sulcus; cs, central sulcus; half, horizontal anterior ramus of the lateral fissure; ifs, inferior frontal sulcus; iprs, inferior precentral sulcus; PF, area PF; PG, area PG; PFG, area PFG; PMCm, middle posteromedial cortex; Pre-SMA, pre-supplementary motor area; pSmG, posterior supramarginal gyrus; SMA, supplementary motor area; STSa, anterior superior temporal sulcus; STSm, middle superior temporal sulcus; STSp, posterior superior temporal sulcus.

Known differences in long-range connectivity patterns of neighboring regions, such as areas 44 and 45, provide a foundation on which to build methods for cortical delineation based on *in vivo* connectivity data. Figure 2.2 summarizes the distinct connectivity patterns of areas 44 and 45, as well as the neighboring area 6VR. Macaque monkey tract-tracing and neuroimaging studies have demonstrated that homologues of these two areas have distinct profiles of connectivity with the

inferior parietal and lateral temporal cortex (Petrides & Pandya, 2002, 2009; Frey et al., 2014; Neubert et al., 2014). These findings are supported by non-invasive tractography studies in the human brain using diffusion MRI (Catani & Jones, 2005; Anwander et al., 2007; Klein et al., 2007; Frey et al., 2008), and functional connectivity based on resting-state fMRI data (Kelly et al., 2010; Margulies & Petrides, 2013).

The dimensionality of high-resolution connectivity data presents many challenges for data exploration and visualization, and current techniques rely on dramatically reducing the dimensionality of the data in order to make sense of them (Margulies et al. 2013). Here, we present the first application of a novel functional connectivity glyph visualization technique (Böttger et al., 2014) that simultaneously displays the connectivity patterns of all possible seed regions in a cortical area, thus allowing for the manual labelling of the extent of areas with homogeneous connectivity patterns and the boundaries between them.

The present study used connectivity priors in conjunction with morphological information to manually delineate the extent and boundaries of areas 44 and 45 at the individual-level. By applying this approach to a large number of subjects, we provide the first probabilistic maps of areas 44 and 45 based on *in vivo* connectivity data.

2.2 Materials and methods

2.2.1 Data

The data used in this study were provided by the Human Connectome Project (HCP). As part of the standard HCP data acquisition protocol, informed written consent was obtained from all participants, and the present study conformed with the World Medical Association Declaration of Helsinki. One hundred and one individuals (59 females; 13 left-handed; mean age 29 years) were selected from the Q3 data release. Additional information regarding selection criteria is

provided in Data S1 and Figure S2.1. These data comprised resting-state fMRI datasets and corresponding T1-weighted structural data for each individual. As part of the default preprocessing pipelines for HCP data, the resting-state fMRI data were denoised by the use of independent component analysis-based artifact removal (Salimi-Khorshidi et al., 2014), and both structural and functional data were registered to HCP 2-mm standard surface space (fs_LR 32k node surfaces). Further details of the standard HCP data acquisition and preprocessing methods can be found in Smith et al. (2013).

2.2.2 Additional data processing

For the current study, it was necessary to conduct additional processing steps to visualize functional connectivity within the left hemisphere of each individual. Approximately 96–98% of individuals are left hemisphere-dominant, and ~70% of left-handed and ambidextrous individuals are left hemisphere-dominant (Rasmussen & Milner, 1975). Of the 101 individuals included in the current study, 13 were left-handed. (i) The functional time-series data of the left cerebral cortex were extracted for each of four 15-min resting-state MRI scans (repetition time 0.7 s) per subject. (ii) Surface-based smoothing with a 2-mm full-width half-maximum kernel was applied. (iii) A correlation matrix was computed and Fisher's r-to-z transformed. (iv) The resulting matrices were averaged across the four resting-state fMRI runs for each participant. (v) The average matrices were z-to-r transformed. (vi) Data were visualized in brainGL[1] by the use of functional connectivity glyphs (Böttger et al., 2014).

2.2.3 Functional connectivity glyphs

Here, we present the first application of functional connectivity glyph visualization as implemented in the open source software brainGL. The connectivity of every point on the cortical surface is presented at each node of the surface-based rendering in a small visual summary called a *functional connectivity glyph* (Figure 2.3). Each glyph represents the distribution of

---

[1] code.google.com/p/braingl

connections from the node to the rest of the cortical surface, with colors indicating the strength of connectivity. By interactive manipulation of various visualization parameters of the glyphs (e.g. size, rotation, color, threshold, and surface inflation), transitions between cortical areas can be made visually explicit.
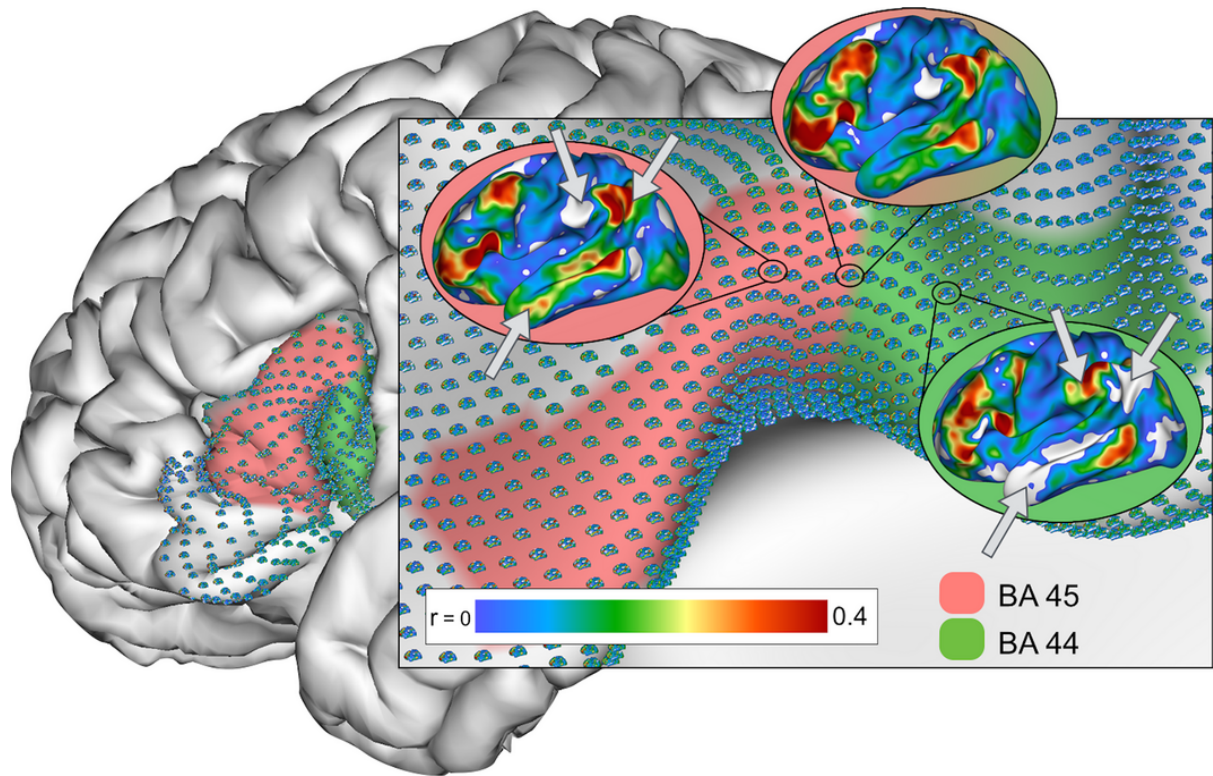
Figure 2.3. Manually labelled areas 45 and 44 for one individual subject on the pial and inflated surfaces with functional connectivity glyphs in the ventrolateral frontal cortex. Each glyph represents the full functional connectivity profile from that node to the rest of the cortical surface. The glyph color indicates the correlation value. As indicated by arrows, connectivity of areas 44 and 45 can be distinguished by differences in the anterior temporal and inferior parietal regions.

2.2.4 Manual delineation procedure

The first step taken in the manual delineation process was to identify the approximate locations of areas 44 and 45 by the use of sulcal landmarks (Figure 2.1). Area 45 is located on the pars triangularis, which is the portion of the inferior frontal gyrus between the horizontal and anterior ascending rami of the lateral fissure, and is dorsally bounded by the inferior frontal sulcus. Area 44 is located on the pars opercularis, which is defined as the portion of the inferior

frontal gyrus that lies ventral to the inferior frontal sulcus and anterior to the inferior precentral sulcus. Rostrally, area 44 is separated from the pars triangularis by the anterior ascending ramus of the lateral fissure. On the basis of these criteria, a large ROI was defined around the inferior frontal gyrus and surrounding areas, and functional connectivity glyphs were rendered for this ROI on the inflated cortical surface representation (Figure 2.3). In order to compensate for variability in the overall connectivity strength between subjects and across cortical areas, the color scale was adjusted to visually normalize the glyph representations. By the use of interactive zooming and manipulation of the glyph parameters, the areas containing glyphs displaying the characteristic connectivity profiles of areas 45 and 44, as described by Margulies & Petrides (2013), were identified and manually labelled. On the lateral surface, area 45 shows strong connectivity with the angular gyrus and the entire extent of the superior temporal sulcus. On the medial wall, there is strong connectivity to the central precuneus region (PGm) and to the cortex anterior to the supplementary motor area. Area 44 shows strong connectivity to the supramarginal gyrus, the anterior part of medial area 6, and the cortex adjacent to the cingulate sulcus, where cingulate motor areas can be identified. Figure 2.2 summarizes the distinct connectivity patterns of areas 44 and 45, and of the neighboring ventrorostral area 6 (6VR).

The two most prominent features used to identify the boundary between the two areas in a posterior direction along the inferior frontal gyrus were: (i) an anterior shift in inferior parietal connectivity from the angular gyrus to the supramarginal gyrus; and (ii) the disappearance of connectivity to anterior and middle temporal regions (Figure 2.3).

The two areas were always labelled as immediately adjacent to each other, so that the posterior boundary of area 45 neighbored the anterior boundary of area 44. If the change in connectivity pattern between the two areas appeared as a gradual transition rather than an abrupt change, the boundary was drawn in the middle of the transition zone.

In some cases, the anterior boundary of area 45 proved difficult to identify, owing to the similarity in the connectivity profiles of area 45 and the neighboring area 47/12. In these subjects, the anterior boundary of area 45 was drawn at the horizontal ascending ramus of the lateral fissure, and not extended anteriorly onto the pars orbitalis.

The posterior boundary of area 44 was primarily defined by identification of a further anterior shift in parietal connectivity to only the most anterior portion of the supramarginal gyrus, and the gradual appearance of connectivity related to the extent of the precentral gyrus. This is consistent with what is known about the functional connectivity of the neighboring area 6VR (Margulies & Petrides, 2013).

The dorsal boundary of area 45 was defined by a shift in connectivity to the anterior temporal and inferior parietal regions very similar to the shift in connectivity found at the boundary between areas 45 and 44. The cortical region immediately dorsal to area 45 is likely to be putative area 9/46v, which has been shown to have similar functional connectivity to areas 44 and 6VR (Margulies & Petrides, 2013).

The dorsal boundary of area 44 was defined by an upward shift in connectivity to parietal regions, covering only the most superior part of the inferior parietal lobule and the extent of the intraparietal sulcus. This cortical region corresponds to cytoarchitectonic area 8AV, and the observed functional connectivity pattern in this area is consistent with results from macaque monkey tract-tracing studies (Petrides & Pandya, 1999).

The ventral boundary of area 45 was primarily defined by a significant drop in overall connectivity values around the anterior portion of the lateral fissure, making precise definition of connectivity differences difficult. This area often suffers from blood oxygen level-dependent signal loss, owing to its proximity to air-filled sinuses (Ojemann et al., 1997).
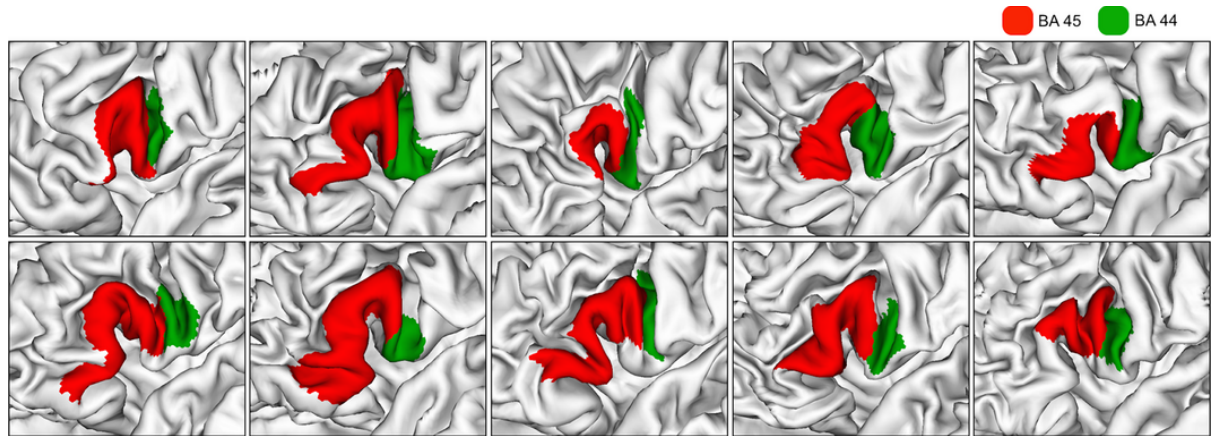
Figure 2.4. Individual manual labels of areas 44 (green) and 45 (red) for 10 randomly selected subjects.

2.2.5 Comparison of functional and cytoarchitectonic probability maps

The individual manual labels (Figure 2.4) were averaged across individuals to create group-level probability maps of the two areas (Figure 2.5). These probability maps were then compared with cytoarchitectonic-based probability maps from the Juelich brain model (Amunts et al., 1999) registered to the same space (fs_LR 32k 440-subject average surface). The probability maps were binarized at various thresholds, and the degree of spatial overlap between them was then computed by use of the Dice coefficient (DC; Dice 1945; Figure 2.6). The DC evaluates the spatial overlap of two samples, A and B, and is defined as:

$$\frac{2|A \cap B|}{|A| + |B|}$$
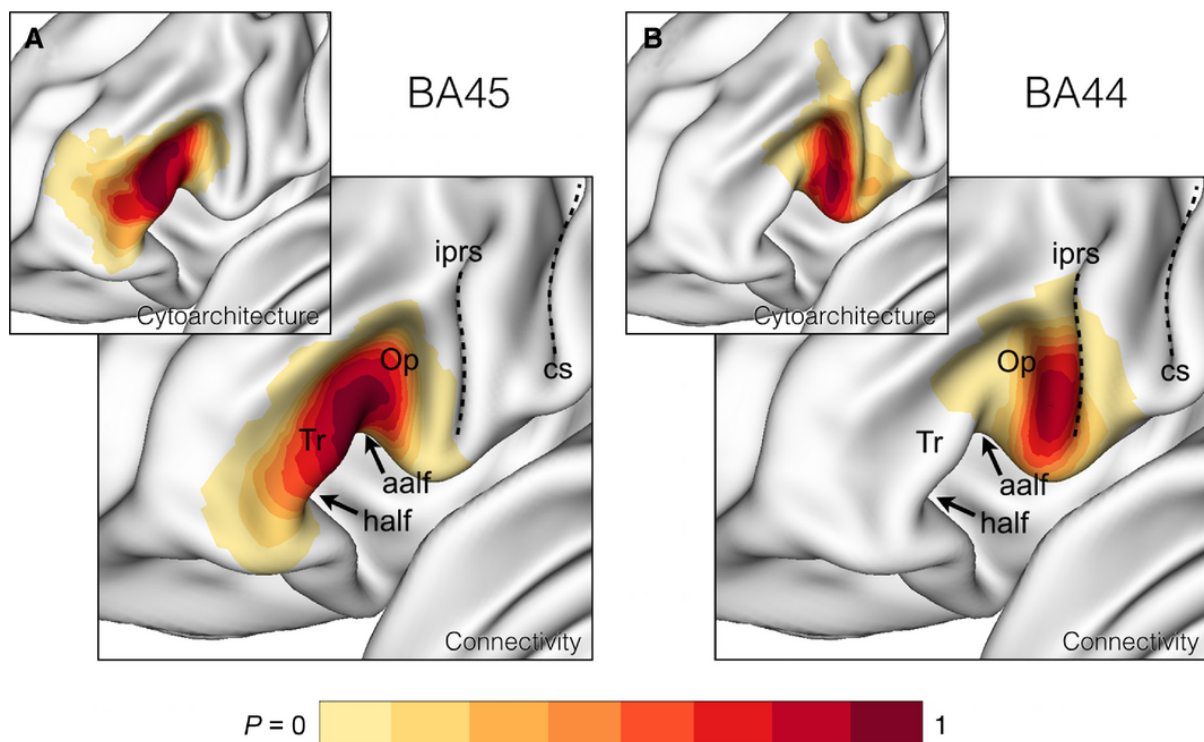
Figure 2.5. Group-average masks of each area across 101 subjects. The color indicates the probability of mask overlap, calculated by averaging across the 101 individual binary area labels. (A and B) Cytoarchitectonic probability maps from the Juelich brain model on the fs_LR 32k 440-subject average surface. In these cytoarchitectonic maps, the colour indicates the probability of overlap of labelled regions across 10 postmortem brains. aalf, anterior ascending ramus of the lateral fissure; cs, central sulcus; half, horizontal anterior ramus of the lateral fissure; iprs, inferior precentral sulcus; Op, pars opercularis; Tr, pars triangularis.
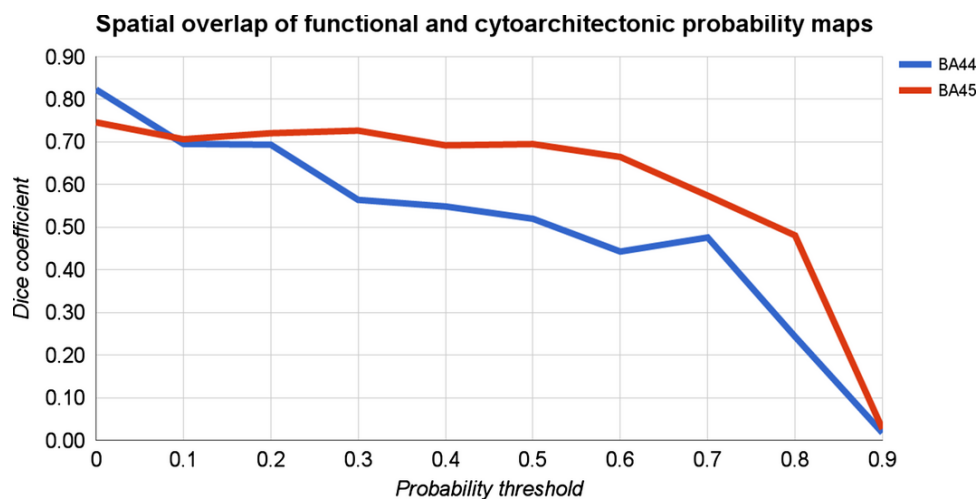
Figure 2.6. Dice similarity of cytoarchitectonic and manual functional connectivity-based probability maps across thresholds. At thresholds of 0.7 and 0.8, the Dice coefficients rapidly decrease, indicating that the peaks of the probability maps do not overlap.

2.2.6 Quantification of sulcal variance

To quantify the individual variability in the morphology of the inferior frontal gyrus, inter-individual sulcal variance was computed by the use of freesurfer *sulc* values, which indicate the depth/height of each node as calculated using the mid-thickness surface (Fischl et al., 1999; Figure 2.7).
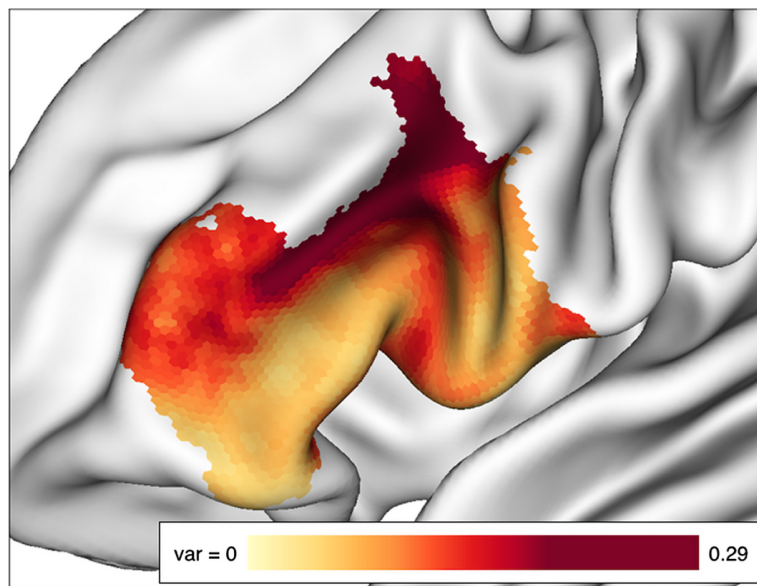
Figure 2.7. Sulcal variance in the ventrolateral frontal cortex across all 101 subjects. The color indicates across-subject variance in the freesurfer 'sulc' variable.

2.2.7 Group-level functional connectivity of manual labels

Group-average functional connectivity maps for each area were created by first computing the average functional connectivity across each individual manual label, and then performing a group-level t-test across the resulting individual maps (voxelwise threshold of $P < 0.001$ with cluster correction of $P < 0.05$) (Figure 2.8).
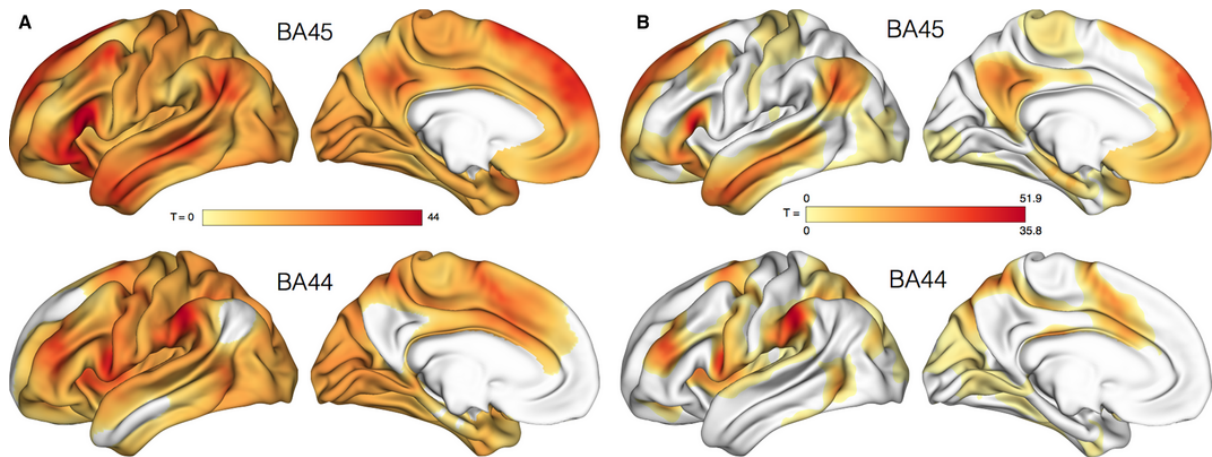
Figure 2.8. Uncontrasted (A) and contrasted (B) group-level functional connectivity maps of areas 44 and 45, with a voxel-wise threshold of P < 0.001 and a cluster threshold of P < 0.05.

2.2.8 Inter-rater and intra-rater reliability of the manual labelling approach

To assess the inter-rater and intra-rater reliability of the manual labelling technique, a subset of the included datasets were re-labelled by the same rater and by a second rater. Ten datasets were randomly selected and labelled by rater 2 according to the same criteria used by rater 1 (described previously). The degree of spatial overlap of the manual labels from rater 1 and rater 2 was then assessed by use of the Dice coefficient (Figure 2.9A). The same 10 datasets were then re-labelled by rater 1 after a period of ~7 months since the first labelling, and the results of the first and second sets of labels were also compared by use of the Dice coefficient (Figure 2.9B).
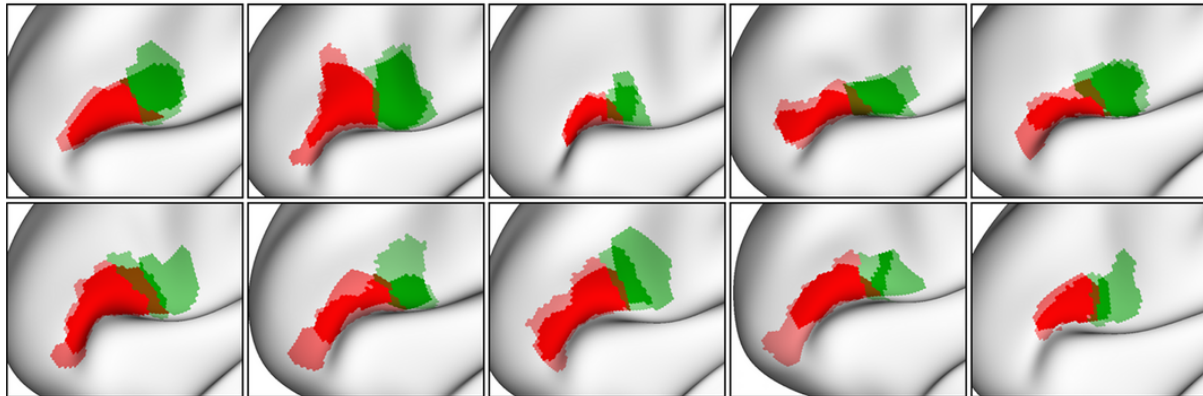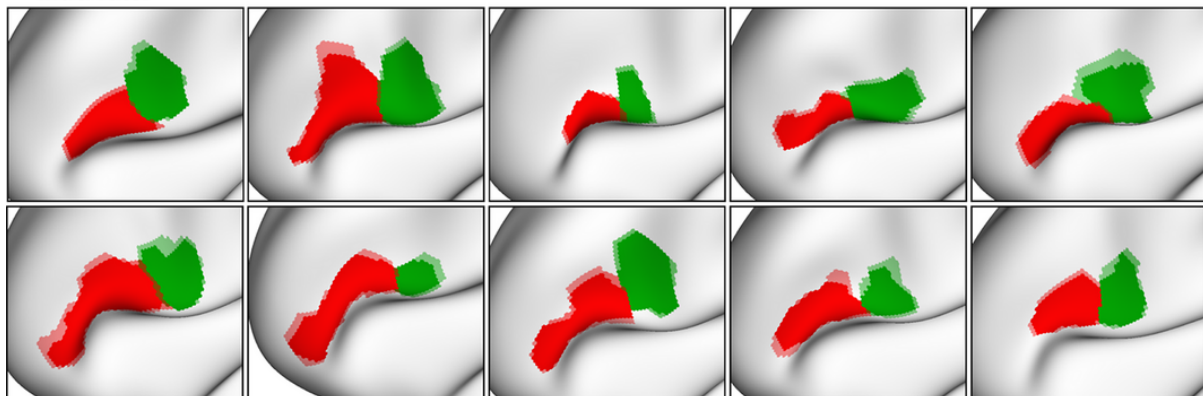
Figure 2.9. (A) Overlap of the area 44 and 45 labels produced by two independent raters for 10 randomly selected datasets. (B) Overlap of the area 44 and 45 labels produced by the same rater at two different time points for the same 10 datasets.

2.2.9 Comparison of manual labelling with automatic clustering

To compare the manual delineation approach with existing automatic parcellation methods, K-means++ and hierarchical Ward clustering were applied to the functional data of an ROI defined by each individual's combined manual area 45 and 44 label. K-means++ is a variant of the standard k-means procedure, with an optimized stochastic seeding technique for selecting the initial cluster centers (Arthur & Vassilvitskii, 2007). Hierarchical clustering with Ward's criterion is a well-established technique for generating functional brain parcels (Murtagh & Legendre, 2011; Thirion et al., 2014).

The clustering procedure was implemented with K = 2 clusters within the manually defined individual areas 44 and 45, by use of the NeuroImaging Analysis Kit for matlab (Bellec et al., 2012). The clustering procedures were based on the Euclidean distance between the connectivity maps associated with two surface nodes. To make the manual and automated labelling approaches directly comparable, each connectivity map was restricted to a manually drawn temporo-parietal mask covering the regions containing features that were used to distinguish the two areas during manual delineation, instead of the full brain an image of the mask is provided in Figure S2.2. The degree of spatial overlap between the manual and automated parcellations was quantified by use of the Dice coefficient, and averaged across the two areas for each subject (Figure 2.10).
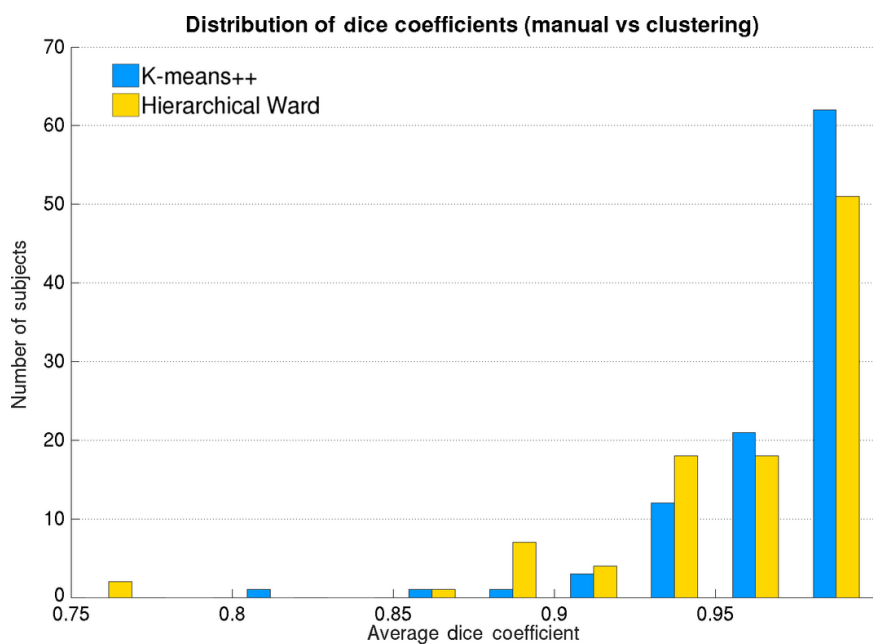
Figure 2.10. Distribution of Dice similarity between manual labels and K-means++ (mean = 0.972) and hierarchical Ward (mean = 0.960) clustering results.

2.3 Results

The 101 individual manual area 44 and 45 labels and corresponding group-level probability maps are freely available for downloading[2]. Examples of individual manual labels for eight randomly selected subjects are shown in Figure 2.4.

2.3.1 Group-level analyses

The group-level probability maps of the manually labelled areas 44 and 45 (Figure 2.5) demonstrate high consistency across all 101 subjects. For area 45, the region of highest overlap between subjects lies on the posterior half of the pars triangularis, directly anterior to the anterior ascending ramus of the lateral fissure. For area 44, the region of highest overlap lies on the anterior bank and fundus of the inferior precentral sulcus, adjacent to and including the pars opercularis. These functional probability maps also show consistency with cytoarchitectonic probability maps derived from postmortem histology (Figure 2.5). The degree of spatial overlap between the functional and cytoarchitectonic probability maps of both areas shows a relatively steady decrease with increasing probability values, with only the highest probability values showing no overlap (Figure 2.6). Figure 2.7 shows a clear increase in across-subject sulcal variance on the pars opercularis, which coincides with the boundary between areas 44 and 45.

As can be seen in Figure 2.8, the group-level connectivity maps clearly reflect the distinct connectivity patterns of areas 44 and 45, with the main distinguishing features being visible in the anterior temporal and inferior parietal regions. Whereas area 45 shows strong connectivity to the anterior portion of the middle temporal gyrus and the angular gyrus, area 44 shows no significant connectivity to these areas. Likewise, area 44 shows the strongest connectivity to the supramarginal gyrus, whereas area 45 shows only very weak connectivity to the most posterior part of this region. Differences can also be seen on the medial wall of the hemisphere, where

---

[2] http://wwwuser.gwdg.de/~cbsarchi/archiv/public/hcp/

area 45 shows strong connectivity with the PGm of the precuneus and a large stretch of the dorsomedial frontal cortex anterior to the supplementary motor area, whereas area 44 shows no connectivity to the PGm, and some connectivity to the cortex adjacent to the cingulate sulcus.

2.3.2 Inter-rater reliability

The overlap between the manual labels of the two raters for all 10 datasets is shown in Figure 2.9A. The average Dice similarities between the labels from rater 1 and rater 2 were 0.53 for area 44 and 0.70 for area 45.

2.3.3 Intra-rater reliability

The overlap between the two sets of labels from rater 1 for all 10 datasets is shown in Figure 2.9B. The average Dice similarities between the first and second sets of labels from rater 1 were 0.89 for area 44 and 0.91 for area 45.

2.3.4 Comparison of manual labelling with automatic clustering

The distribution of average Dice similarity between the manual labels and the clustering results is shown in Figure 2.10. K-means++ produced cluster solutions with higher spatial overlap than hierarchical Ward clustering. The high values for both clustering algorithms can be accounted for by the a priori matching of the input ROI, which was defined by the manual labels. Figure 2.11 shows the subject with the highest discrepancy between the results of the manual labelling and K-means++ clustering (lowest DC). There are two mismatch areas, the first of which coincides with the boundary between areas 45 and 44. The connectivity pattern in this area suggests a gradual transition rather than an abrupt boundary between the two areas. The second mismatch area lies towards the anterior end of the manually labelled area 45. This area shows a slight change in parietal connectivity as compared with the rest of the manually labelled area 45, which may have contributed to the difference in the clustering results. However, because of the anatomical location of the region and the presence of other connectivity features (such as strong

connectivity along the superior temporal gyrus), the area was included in the manual area 45 label. In cases such as these, automatic clustering algorithms may benefit from a region-growing approach or spatial constraints in order to avoid anatomically separate regions being assigned to the same cluster (Craddock et al., 2012; Blumensath et al., 2013; Wig et al., 2014a).
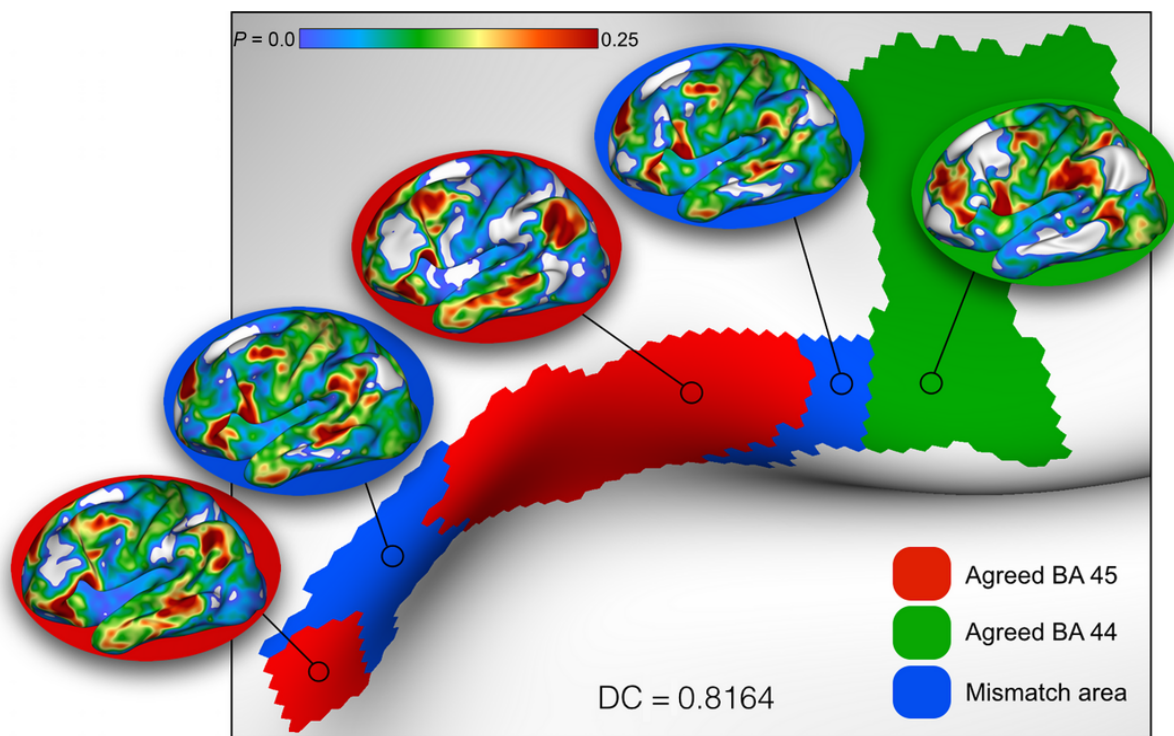
Figure 2.11. Manual area 44 and 45 labels and K-means++ clustering results for the subject with the lowest spatial overlap (DC=0.8164). The red and green regions mark agreement between the manual and clustering results, and the blue regions show areas of mismatch. Sample glyphs are shown for each region.

2.4 Discussion

In the present study, we manually parcellated Broca's region in individual brains *in vivo*. By using functional connectivity glyph visualization, we were able to delineate the boundaries of areas 44 and 45 in 101 individual brains from the HCP on the basis of morphological and connectivity criteria. The manual labelling technique showed good test–retest reliability, as shown by the spatial overlap of the manual labels produced by the same and independent raters. The group-level comparisons are consistent with previous knowledge about the structure and connectivity

of these areas. These findings validate the utility of functional connectivity glyph visualization for individual-level cortical parcellation and, in addition, provide further evidence for the distinct connectivity profiles of areas 44 and 45 in the human brain.

Our manual labelling produces group-level probability maps that show a high degree of consistency with cytoarchitectonic probability maps of the same areas (Figures 2.5 and 2.6). However, it is interesting to note the slight differences in the anatomical locations of the areas of maximum probability between modalities. The area of maximum probability for the functional connectivity-based map of area 44 lies within the fundus of the inferior precentral sulcus, which is slightly posterior to its location on the anterior wall of the inferior precentral sulcus, as described by the probabilistic cytoarchitectonic map. Similarly, the area of maximum probability for the functional map of area 45 lies on the posterior half of the pars triangularis, whereas the cytoarchitectonic map's maximum overlap region is shifted anteriorly towards the middle of the pars triangularis. Although the present study included 101 high-resolution *in vivo* resting state fMRI datasets, the cytoarchitectonic maps are based on only 10 postmortem brains, which may not be a large enough sample to capture inter-individual variability in the locations of these areas. Additionally, both modalities rely heavily on a variety of registration techniques, which could help to explain the observed differences. Another possible reason for the shift towards the fundus of the inferior precentral sulcus in the functional connectivity-based map of area 44 is the contribution of large draining veins, which tend to lie along sulci, to the blood oxygen level-dependent signal measured with fMRI techniques (Krings et al., 1999). Nonetheless, such discrepancies between probability maps from different modalities could have important implications for the way in which areas 44 and 45 are currently defined, both functionally and structurally.

The group-average connectivity maps (Figure 2.8) reflect consistency in the unique connectivity patterns of areas 44 and 45 across subjects, and highlight the main distinguishing features in the

anterior temporal and inferior parietal regions. These results are consistent with the findings of previous studies investigating the connectivity differences between areas 44 and 45 (Petrides & Pandya, 2009; Kelly et al., 2010; Margulies & Petrides, 2013). Although there is strong evidence for the correspondence between measures of functional and structural brain connectivity (Damoiseaux & Greicius, 2009), it is important to keep in mind that the relationship between resting-state functional connectivity and anatomical connectivity is not one-to-one. Functional connectivity has been observed between regions where no direct anatomical connection exists (Vincent et al., 2007; Honey et al., 2009; Miranda-Dominguez et al., 2014), which may reflect indirect connectivity between regions. An example of this in the current study is the presence of functional connectivity between the precuneus and area 45 (Figures 2.2 and 2.8), where no direct anatomical connectivity exists. However, the PGm is connected with area PG of the inferior parietal lobule. This finding is consistent with previous studies using resting-state fMRI to investigate the functional connectivity of area 45 (Margulies & Petrides, 2013).

The group-level contrasted connectivity map of area 44 (Figure 2.8B) shows strong functional connectivity to the anterior, but not to the posterior, part of the supramarginal gyrus. This is most likely attributable to area 45 also showing some connectivity to the posterior supramarginal gyrus in addition to the expected connectivity to the angular gyrus, as can be seen in the uncontrasted map (Figure 2.8A). This overlap will have led to the posterior supramarginal connectivity not showing up in the contrasted group-level map for area 44. However, this result could also be indicative of the inherent difficulty in distinguishing the very subtle differences in the connectivity patterns of areas 44 and the neighboring premotor area 6VR, which shows strong connectivity to only the most anterior part of the supramarginal gyrus, and may have led to parts of area 6VR being included in the BA 44 labels for some subjects. Additionally, it has been suggested that the cytoarchitectonically defined area 44 is not functionally homogeneous, and can be further subdivided into five distinct clusters by the use of meta-analytic connectivity-based parcellation (Clos et al., 2013). Whereas the current study focused on inter-areal

differences in connectivity patterns, more subtle intra-areal differences may also exist and contribute to the results.

2.4.1 Comparison with clustering results

Although both hierarchical Ward and K-means++ clustering produced results with a high degree of spatial overlap with the manual labels (as measured by use of the Dice coefficient), K-means++ resulted in a slightly higher average Dice similarity across subjects, and also fewer subjects with low spatial overlap between modalities (Figure 2.10). The areas of discrepancy between the automatic and manual area labels in individual subjects (Figure 2.11) often coincide with regions within which the connectivity shifts gradually from one pattern to another over the width of several cortical nodes. Further research is needed to investigate how this relates to the underlying cortical boundaries and transitions within these regions. Additionally, investigation of these discrepancies between automatic and manual parcellation results may prove useful in identifying additional features that could be utilized to more effectively distinguish the areas. The second area of discrepancy highlighted in Figure 2.11 is one common to many of the subjects with low Dice similarity between the automatic and manual labels, and demonstrates an advantage of the manual labelling approach over the chosen automatic parcellation algorithms. Whereas the manual labelling approach imposes a spatial constraint on the results by always producing exactly two continuous regions corresponding to areas 44 and 45, the automatic parcellation techniques sometimes produce discontinuous clusters, owing to subtle inhomogeneities in the connectivity pattern within an otherwise homogeneous region. For this reason, automatic clustering algorithms may benefit from a region-growing approach or the implementation of spatial constraints in order to avoid anatomically separate regions being assigned to the same cluster (Bellec et al., 2006; Craddock et al., 2012; Blumensath et al., 2013; Wig et al., 2014a). Although we chose to use versions of K-means and hierarchical clustering, owing to their prevalence, more sophisticated algorithms, such as consensus clustering (Goder & Filkov, 2008), exist that may perform better within the given framework.

One of the implicit challenges of existing automatic clustering techniques when applied to fMRI data is determining the proper number of clusters to output, with the aim of producing functionally meaningful results. The K-means clustering algorithm requires a priori input of k, the number of clusters, to split n, the number of voxels (in this case, surface nodes). Hierarchical clustering attempts to avoid this problem by outputting a hierarchical dendrogram that spans from all observations being in the same cluster, to all observations being separated across distinct clusters. However, a decision must still be made post hoc on which level of the dendrogram to use to interpret the results. In contrast, our manual delineation method defines the number of clusters on the basis of prior knowledge of the areas of interest. Specific to the present study, a rough anatomical ROI corresponding to Broca's region is split into exactly two clusters, corresponding to areas 44 and 45.

Most automatic clustering algorithms, such as K-means and hierarchical clustering, produce binary results, whereby each data element is assigned to only one cluster. When applied to cortical parcellation, this can lead to the interpretation of sharp boundaries between cortical areas, which are not necessarily reflected in the data. As has recently been demonstrated with boundary detection techniques, some neighboring cortical areas show sharp boundaries with abrupt changes in functional connectivity, whereas others gradually transition from one connectivity pattern to the next over a larger cortical region (Wig et al., 2014b). Attempts have been made to address this issue by the development of so-called fuzzy clustering techniques, in which data elements can belong to more than one cluster and are assigned multiple membership values (Yoon et al., 2003; Nock & Nielsen, 2006). Our manual labelling approach offers a novel method for addressing this issue. In the present study, areas 44 and 45 were labelled in a binary manner, with each node belonging to only one cluster, in order to facilitate comparison with clustering results. However, the manual labelling tools implemented in brainGL also allow for labelling of areas with non-binary values. This tool could easily be used to indicate uncertainty

regarding the probability of a particular data point belonging to a certain area, or to label transition zones on the basis of visually observable changes in the glyphs.

2.4.2 Individual-level parcellation

Owing to the high degree of individual variability in the cortical morphology of brain regions such as Broca's region (Figure 2.7), individual-level analysis is necessary to produce accurate cortical parcellations. This is demonstrated by the difficulties encountered in previous studies aimed at determining connectivity differences between subregions of the ventrolateral frontal cortex at the group level (Kelly et al., 2010). The current gold standard for individual-level cortical parcellation is considered by many to be the cytoarchitectonic definition of regions in postmortem brain tissue, but no comparable method exists for *in vivo* data. By making use of high-quality resting-state fMRI data, our manual delineation method provides a much-needed improvement on existing methods for individual-level *in vivo* cortical labelling. Such an approach also facilitates the investigation of the relationship between individual differences in cortical organization and behavioral phenotypes.

2.4.3 Clinical applications

The ability to accurately define the location and extent of particular functional regions in the individual living human brain without the need for behavioral tasks would be beneficial for highly sensitive clinical applications such as neurosurgical planning. For example, such a technique could be used to ensure the preservation of language functions known to be associated with areas 44 and 45 in patients requiring surgery in the ventrolateral frontal cortex. To our knowledge, no behavioral task exists that is able to reliably distinguish areas 44 and 45 from each other, and, in a clinical context, such a task might in any case be too demanding for the patient. In contrast, the use of resting-state fMRI is suitable and undemanding for patients of all kinds. Additionally, existing visualization techniques for resting-state fMRI are not sufficient for precise individual-level delineation of cortical areas. Although seed-based

connectivity visualization allows for the identification of distinct connectivity patterns of single ROIs, it does not provide a method with which to map the extent and boundaries of the cortical areas to which the chosen seed regions belong. Functional connectivity glyph visualization addresses this issue by comparing the connectivity patterns of multiple neighboring seed regions simultaneously, facilitating parcellation of areal boundaries. This approach could, of course, be extended beyond Broca's area to distinguish and parcellate any regions of the brain with distinct functional connectivity profiles and various clinical implications.

Although the current study made use of a dataset with very unique scanning parameters (1 hour of data per subject at high spatial resolution), such high-quality data are not required for our manual delineation approach. It has been shown that scan times as low as 5 min result in stable estimates of correlation strengths (Van Dijk et al., 2010), and that improvements in inter-session and intra-session reliability plateau at 9–12 min and 12–16 min respectively (Birn et al., 2013). On the basis of this knowledge, we believe that our manual delineation technique is applicable to resting-state data acquired under the constraints of a clinical setting.

2.4.4 Manual parcellation as a precursor to automated methods

Existing automatic parcellation techniques are data-driven, and do not take into account the large amount of prior knowledge that exists about the anatomy and connectivity of particular brain regions, making it difficult to evaluate the validity and accuracy of their results. For example, although boundary detection approaches (Cohen et al., 2008; Hirose et al., 2009, 2012) are powerful tools for identifying transitions between cortical regions, the resulting gradient maps do not contain any information about the nature or location of the changes underlying the detected boundaries. Our manual labelling approach attempts to address this issue by incorporating prior knowledge of the anatomical location and variability of the ROIs, and basing each individual parcellation on known differences in the areas' distinct connectivity profiles. The resulting area labels therefore provide a valuable basis for the subsequent development of automated

parcellation approaches with comparable precision at the individual level. For example, the manually labelled datasets could be used as input for feature selection and pattern classification algorithms. A corresponding approach has been used previously for an automated cortical labelling method based on gyral patterns (Desikan et al., 2006). Similarly, the group-level probability maps could also be used to enforce a spatial constraint on the outputs of existing clustering techniques.

2.4.5 Conclusions

The results of the present study validate the use of functional connectivity glyph visualization for manual cortical parcellation at the individual level. Although this approach does not replace the need for automated cortical parcellation techniques, it fills a much needed gap in the available tools for mapping cortical anatomy on the basis of connectivity data. Future work will build on the present study by making use of the manually labelled datasets for the development of an automated cortical parcellation of areas 45 and 44 based on morphological and connectivity information. Additionally, the individual-level parcellations provide an opportunity to categorize morphological variability in functionally defined regions between subjects, which was not addressed in the current study. The manual labels of areas 44 and 45 from the current study have been made openly available[3] to facilitate further investigation, comparison with results from other methods, and the more extensive development of computationally driven parcellation techniques.

---

[3] wwwuser.gwdg.de/~cbsarchi/archiv/public/hcp/

2.5 Supporting information

2.5.1 Exclusion criteria

The 101 subjects included in the current study were selected according to the following protocol. 125 individuals were randomly selected from the HCP Q3 data release. Of the 125 datasets, 9 were subsequently excluded due to missing resting-state fMRI runs. The remaining datasets were then visually inspected and subjects with abnormally high or spatially variable average r-values were excluded (Figure S2.1). This resulted in 101 healthy individuals (59 females; 13 left-handed; mean age = 29;) being included in the current study.
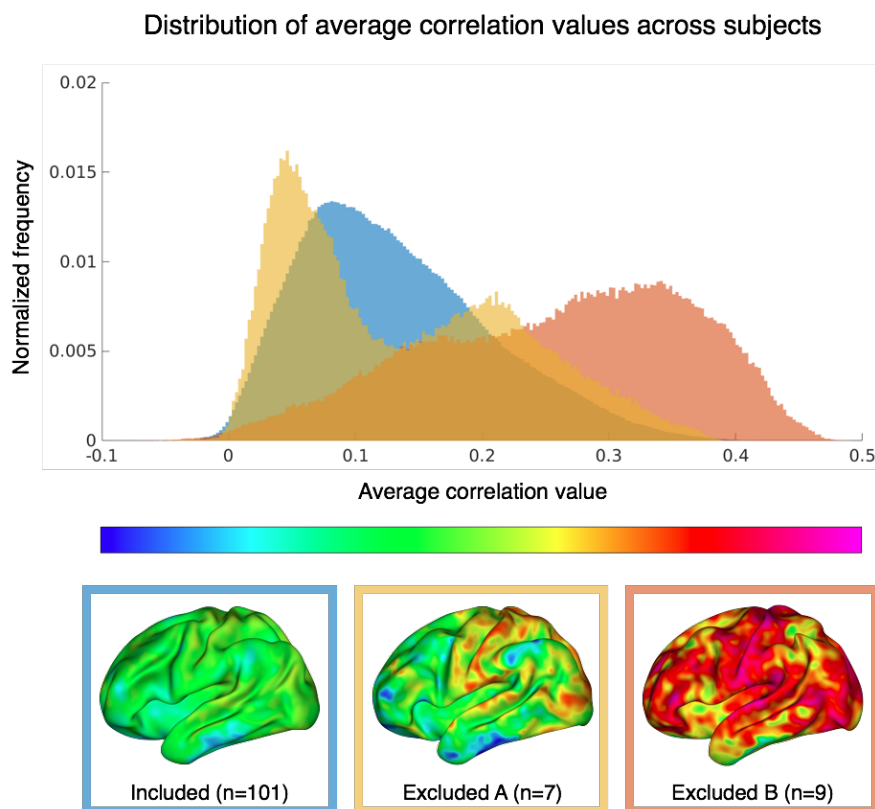
Figure S2.1: Top: Distribution of correlation values in all subjects included (blue - Included) and excluded due to extremely variable (yellow - Excluded A) or high (red - Excluded B) values. Bottom: Average correlation values across the cortical surface of one representative individual from each subject group.

2.5.2 Masking of clustering results

A temporo-parietal mask (Figure S2.2) was used to constrain the described clustering analyses. The ROI was manually drawn on a group-average surface representation and then used to constrain the connectivity maps of the individual datasets prior to clustering.

Figure S2.2: Temporo-parietal mask used to constrain clustering results.

2.5.3 Comparison of manual labeling to automatic clustering

In addition to the automatic clustering results presented, several variations of the standard K-means and Hierarchical clustering algorithms were run in order to evaluate which version would produce results most similar to the manual labels. This included standard K-means, K-means++, which provides improved initial cluster center selection, and Hierarchical clustering with and without Ward's criterion. Additionally, K-means++ and Hierarchical Ward clustering were run with and without application of a temporo-parietal mask (constrained).

As described, the clustering was run with K=2 on the individual-subject left-hemisphere correlation matrices using the NeuroImaging Analysis Kit (NIAK) for Matlab (Bellec et al. 2012). For the constrained runs, each correlation matrix was constrained by a temporo-parietal mask covering the regions containing features that were used to distinguish the two areas during manual delineation prior to clustering. The degree of spatial overlap between each of the manual

labels and the clustering results was then calculated using the Dice coefficient and averaged

across the two areas for each subject (Figure S2.3).
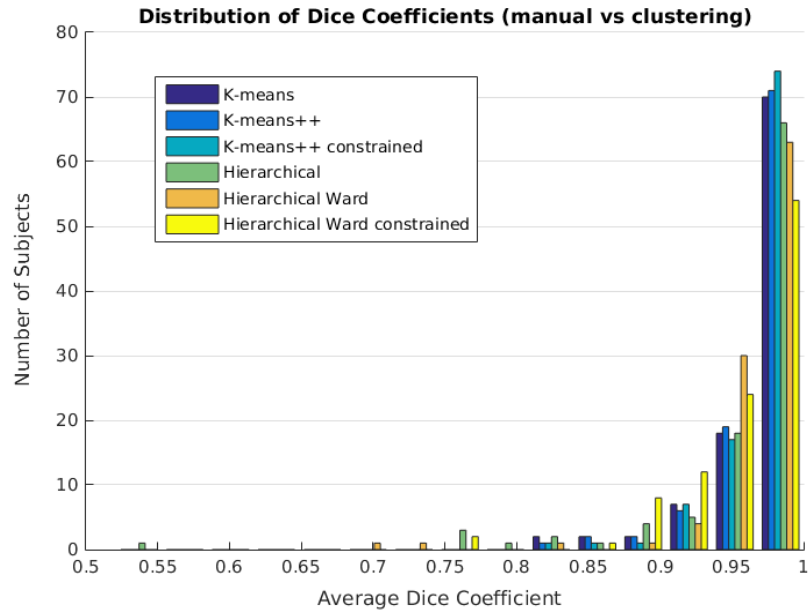
Figure S2.3: Distribution of Dice similarity between manual labels and K-means (mean = 0.967), K-means++ (mean = 0.969), K-means++ constrained (mean = 0.972), Hierarchical (mean = 0.955), Hierarchical Ward (mean = 0.953), and Hierarchical Ward constrained (mean = 0.960) clustering results.

Chapter 3 - Automated individual-level parcellation of Broca's region based on functional connectivity

Abstract

Broca's region can be subdivided into its constituent areas 44 and 45 based on established differences in connectivity to superior temporal and inferior parietal regions. The current study builds on our previous work manually parcellating Broca's area on the individual-level by applying these anatomical criteria to functional connectivity data. Here we present an automated observer-independent and anatomy-informed parcellation pipeline with comparable precision to the manual labels at the individual-level. The method first extracts individualized connectivity templates of areas 44 and 45 by assigning to each surface vertex within the ventrolateral frontal cortex the partial correlation value of its functional connectivity to group-level templates of areas 44 and 45, accounting for other template connectivity patterns. To account for cross-subject variability in connectivity, the partial correlation procedure is then repeated using individual-level network templates, including individual-level connectivity from areas 44 and 45. Each node is finally labeled as area 44, 45, or neither, using a winner-take-all approach. The method also incorporates prior knowledge of anatomical location by weighting the results using spatial probability maps. The resulting area labels show a high degree of spatial overlap with the gold-standard manual labels, and group-average area maps are consistent with cytoarchitectonic probability maps of areas 44 and 45. To facilitate reproducibility and to demonstrate that the method can be applied to resting-state fMRI datasets with varying acquisition and preprocessing parameters, the labeling procedure is applied to two open-source datasets from the Human Connectome Project and the Nathan Kline Institute Rockland Sample. While the current study focuses on Broca's region, the method is adaptable to parcellate other cortical regions with distinct connectivity profiles.

3.1 Introduction

Broca's region is one of the most widely studied brain areas because of its historical significance and critical role in language processing (Sahin et al. 2009). Located on the inferior frontal gyrus in the language-dominant hemisphere, it can be subdivided into its constituent areas 44 and 45 based on cytoarchitectonic boundaries that roughly correspond to the macroanatomical landmarks of the pars opercularis and pars triangularis respectively (Amunts et al. 1999; Petrides and Pandya 2002). Based on this knowledge, it is common in neuropsychological research to make use of morphologically defined ROIs as proxies for areas 44 and 45. However, there is a high degree of inter-individual variability in cortical morphology in the ventrolateral frontal region (Tomaiuolo et al. 1999; Keller et al. 2007), making it difficult to distinguish accurately areas 44 and 45 based on macroanatomical features alone. In addition to anatomical variability, recent studies using resting-state fMRI have shown that higher-level cortical association areas, including Broca's region, show particularly strong inter-individual variability in functional connectivity (Yeo and Krienen et al. 2011; Mueller et al. 2013; Wig et al. 2014a). For these reasons, tailoring cortical parcellation approaches to the individual brain (see for example Wang et al. 2015) is critical in order to capture the unique functional and morphological characteristics of each subject with precision. Functional atlases based on individual-level parcellation provide a foundation for exploring the relationship between structural and functional boundaries in the brain and their correspondence across individuals.

Existing automatic connectivity-based parcellation techniques aim to provide whole-brain functional atlases by parcellating the entire cerebral cortex using the same basic criteria, namely similarity or homogeneity of connectivity patterns, and therefore do not take advantage of the considerable amount of prior knowledge that exists about the anatomy and unique connectivity patterns of highly studied regions such as areas 44 and 45. Additionally, since no gold-standard connectivity-based cortical atlas currently exists, difficulty can arise when interpreting the

correspondence of whole-brain parcellations to existing ontologies. For this reason, anatomical criteria are commonly used to define cortical regions in studies using functional data. The anatomy-informed manual labeling approach for areas 44 and 45 described in the previous chapter attempts to address this issue by incorporating prior knowledge of the anatomical locations, distinct connectivity profiles, and variability of the ROIs into each individual parcellation. It has previously been shown that areas 44 and 45 are clearly distinguishable by differences in connectivity to the inferior parietal and lateral temporal regions using resting-state functional connectivity (Kelly et al. 2010; Margulies and Petrides 2013). Based on these connectivity differences, Brodmann areas 44 and 45 were manually labeled in 101 individual datasets using functional connectivity glyphs (Boettger et al. 2014; Jakobsen et al. 2016). By simultaneously displaying the seed-based connectivity patterns of multiple neighboring vertices of the cortical surface reconstruction, this technique allows for meticulous manual segmentation based on differences in the connectivity patterns of adjacent cortical regions. Resulting group-level probability maps based on the individual manual parcellations of areas 44 and 45 are consistent with cytoarchitectonic probability maps of the same regions while still reflecting the high degree of individual morphological variability, thereby validating the usefulness of intrinsic functional connectivity as the basis for accurate *in vivo* cortical parcellation. The manually defined area labels therefore serve as gold-standard functional labels that can be used to validate the results of an automated data-driven parcellation approach.

The current study presents a new method for automated, observer-independent, and anatomy-informed cortical parcellation based on functional connectivity. This method aims to simulate the manual parcellation procedure and takes advantage of prior knowledge of well-studied brain regions by basing parcellations on a combination of area-specific functional connectivity features and meaningful anatomical criteria. Using the previously generated manual labels of areas 44 and 45 as gold-standard, the goal of this approach is to generate observer-independent area labels with comparable precision to manual labeling at the individual-level. The approach consists of

three main steps: (1) defining a broad target ROI that includes nodes surrounding the areas of interest, (2) assessing the unique similarity of each node's connectivity to a set of templates corresponding to the areas of interest and other canonical networks, and (3) weighting the similarity values by spatial location and ensuring spatial continuity of the final labels. In keeping with the manual parcellation procedure, the automated parcellation pipeline incorporates macroanatomical information through ROI definition and spatial weighting, but allows the resulting functional boundaries to deviate from anatomical constraints in order to better fit the individual anatomy and connectivity.

The area 44 and 45 labels derived from the automated observer-independent parcellation method display a high degree of overlap with the results of the manual labeling procedure, validating the precision of the method at the individual-level. Parcellation results are also presented for an independent resting-state fMRI dataset, demonstrating that the method is able to generalize to datasets with varying acquisition and preprocessing parameters.

3.2 Materials and methods

3.2.1 Data and preprocessing

The data used in the development of the parcellation pipeline were provided by the Human Connectome Project (HCP) and comprised 101 previously manually labeled (based on connectivity and anatomical priors) resting-state fMRI datasets and corresponding T1-weighted structural data for each individual (mean age 29, 13 left-handed, 59 females). All data were preprocessed according to standard HCP preprocessing pipelines including ICA-based artefact removal (Salimi-Khorshidi et al. 2014) and registration to HCP 2mm standard surface space (fs_LR 32k node surfaces). Further details about the standard HCP data acquisition and preprocessing methods can be found in Smith et al. (2013). Since language processing is strongly left-lateralized (Rasmussen and Milner 1975), analyses included only the left cerebral hemisphere.

Several additional study-specific preprocessing steps were performed as follows: (1) The functional time-series data of the left cerebral cortex was extracted for each of four 15-minute rfMRI scans (TR = 0.7s) per subject, (2) surface-based smoothing with a 2mm FWHM kernel was applied, (3) a correlation matrix was computed and Fisher's r-to-z transformed (Fisher 1915; 1921), (4) the resulting 32k x 32k matrices were averaged across the four rfMRI runs for each participant, (5) the average matrices were z-to-r transformed. Note that these datasets are identical to those used in the previous chapter describing the manual labeling procedure.

In order to show that the parcellation pipeline can be successfully applied to independent datasets, 100 additional resting-state and corresponding T1-weighted structural datasets from the Enhanced Nathan Kline Institute- Rockland Sample (NKI) (Nooner et al. 2012) (mean age 43, 10 left-handed, 65 females) were also used. These data comprised one 10-minute multiband rfMRI scan (TR = 645ms) per subject, for which the following preprocessing steps were performed: (1) removal of the first 5 volumes, (2) head motion correction, (3) coregistration of functional data to anatomy, (4) denoising, and (5) band-pass filtering. The full preprocessing pipeline for this dataset can be found online[4]. Several additional study-specific preprocessing steps were then performed as follows: (6) The timeseries data of the left cerebral cortex were extracted and projected to fsaverage5 (10k nodes per hemisphere) surface space, (7) surface-based smoothing with a 6mm FWHM kernel was applied. The choice of a more traditional 6mm smoothing kernel was due to the larger voxel size and shorter resting-state acquisition time of the NKI as compared to the HCP data. (8) Correlation matrices were then computed using Pearson's correlation, and (9) the individual native FreeSurfer surfaces were downsampled to fsaverage5 template for visualization purposes.

---

[4] github.com/NeuroanatomyAndConnectivity/nki_nilearn

3.2.2 Generation of connectivity templates and ICA maps

Prior to parcellation of the individual datasets, group-level connectivity maps of areas 44 and 45 (Figure 3.1) were computed based on the 101 manually labeled HCP datasets. First, the average functional connectivity was averaged across all vertices included in each individual manual label, and the resulting connectivity vectors were then averaged across the 101 individuals. These connectivity maps were subsequently used as group-level seed-based functional connectivity templates for areas 44 and 45 in the individual-level parcellation pipeline.
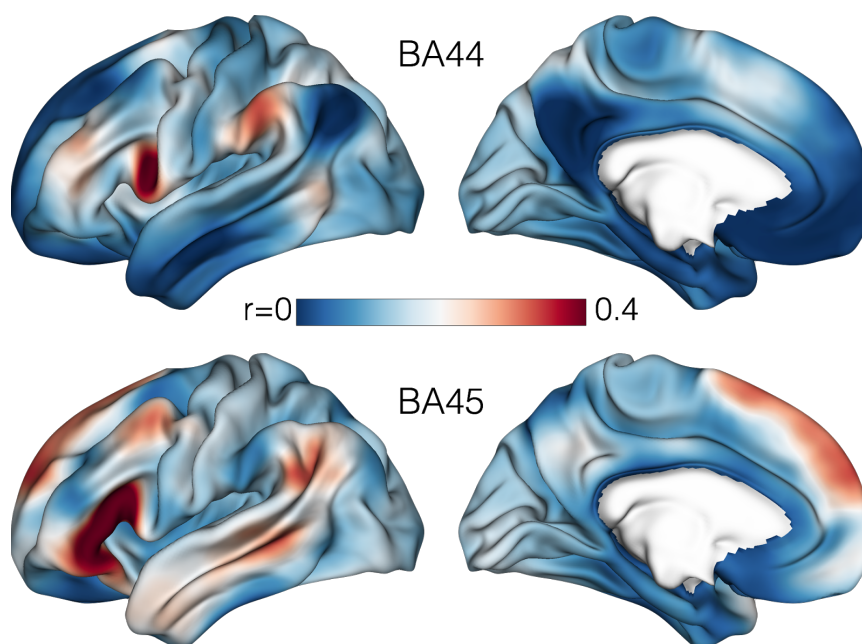
Figure 3.1: Group-level connectivity maps of areas 44 and 45 based on the average connectivity from 101 manually labeled functional connectivity datasets. These maps were used as group-level seed-based connectivity templates in the automated parcellation pipeline. Note the connectivity differences in the anterior temporal and inferior parietal regions.

In order to estimate the possible connectivity patterns of vertices not belonging to areas 44 or 45, group- and individual-level independent component analyses (ICA) were run on the timeseries of the 101 HCP datasets, resulting in 20 group- and individual-level independent component maps (Figures 3.2 and 3.3 respectively).

Spatial correlations were then computed between each of the group-level IC maps and the previously generated group-level connectivity templates of areas 44 and 45 (Figure 3.1). The two IC maps with the highest spatial correlations (r>0.4) were then removed to ensure that only IC maps not representative of areas 44 and 45 were included. The 18 remaining IC maps were subsequently used in the parcellation pipeline as group-level templates representing the connectivity patterns of vertices located outside of areas 44 and 45. A similar procedure applied to the individual-level IC maps is included in the parcellation pipeline, described below.

Figure 3.2: Results from the 20-component group-level ICA of the 101 HCP datasets. Component maps with the highest spatial correlation with the group-level seed-based connectivity templates of areas 44 and 45 were removed (outlined in red), and the remaining component maps were used in the automated parcellation pipeline.

3.2.3 Parcellation pipeline

The individual datasets were then processed using an automated parcellation pipeline to produce binary labels of areas 44 and 45 tailored to account for intersubject variability in functional connectivity patterns by first comparing the connectivity of single vertices to group-level templates and then refining the results using individual-level connectivity patterns. The pipeline comprised 7 steps, as summarized in Figure 3.4:

1. To reduce the size of the input matrix and thereby increase the processing speed of the parcellation pipeline, the whole-brain connectivity matrix of each individual subject is masked along one dimension to an ROI covering the ventrolateral prefrontal cortex, resulting in an asymmetrical matrix representing the connectivity of each vertex within the ROI to the whole cortical surface. As a result, only vertices within the ROI will be labeled. To allow for a higher degree of morphological variability than would be provided by anatomical labels based on sulcal information alone, the ROI is created by combining the FreeSurfer labels corresponding to the pars opercularis and pars triangularis with binarized (probability>0) cross-subject probability maps of areas 44 and 45 based on the 101 manually labeled datasets.

2. Vertex-wise partial correlations are then run for the two group-level seed-based connectivity templates for areas 44 and 45. In this step, the connectivity pattern of each vertex is correlated with each of the template connectivity maps, regressing out the effects of the eighteen remaining group-level IC maps and the adjacent area 44 or 45. This results in two partial correlation maps representing the similarity of the connectivity patterns of each vertex within the ROI to the group-level seed-based connectivity templates for areas 44 and 45.

3. The vertices with the maximum partial correlation to the group-level connectivity templates for areas 44 and 45 are then identified as the vertices with the connectivity patterns most representative of areas 44 and 45. The seed-based connectivity vectors corresponding to these representative vertices are then extracted from the connectivity

matrix and subsequently used as individual-level seed-based connectivity templates for areas 44 and 45.

4. Spatial correlations are then computed between each of the individual-level IC maps and the individual-level seed-based connectivity templates for areas 44 and 45 generated in step 3. The IC maps with the highest spatial correlations ($r>0.4$) are then removed (Figure 3.3). To account for individual variability in connectivity patterns, vertex-wise partial correlations are then run for the two individual-level seed-based connectivity templates for areas 44 and 45 and all remaining individual-level IC component maps. This step results in a set of partial correlation maps representing the similarity of the connectivity patterns of each vertex within the ROI to each of the individual-level connectivity template maps (consisting of areas 44 and 45, and approximately 18 IC maps for a typical subject).

5. A spatial weighting is then applied in order to decrease the probability of vertices falling outside a certain anatomical region being included in the final labels for areas 44 and 45. This step consists of multiplying the new individual-level partial correlation maps for areas 44 and 45 by the common logarithm of the cross-subject spatial probability maps of areas 44 and 45 based on the 101 manually labeled datasets. The common logarithm is applied in order to decrease the slope of the probability maps and thereby apply a less restrictive spatial constraint.

6. A winner-take-all partition is then run across all partial correlation maps, resulting in each vertex within the ROI being assigned to one of approximately 20 possible connectivity-based classes.

7. To ensure spatial continuity of the final labels, the largest clusters assigned to the classes corresponding to areas 44 and 45 are then extracted, forming the final binary labels of areas 44 and 45.
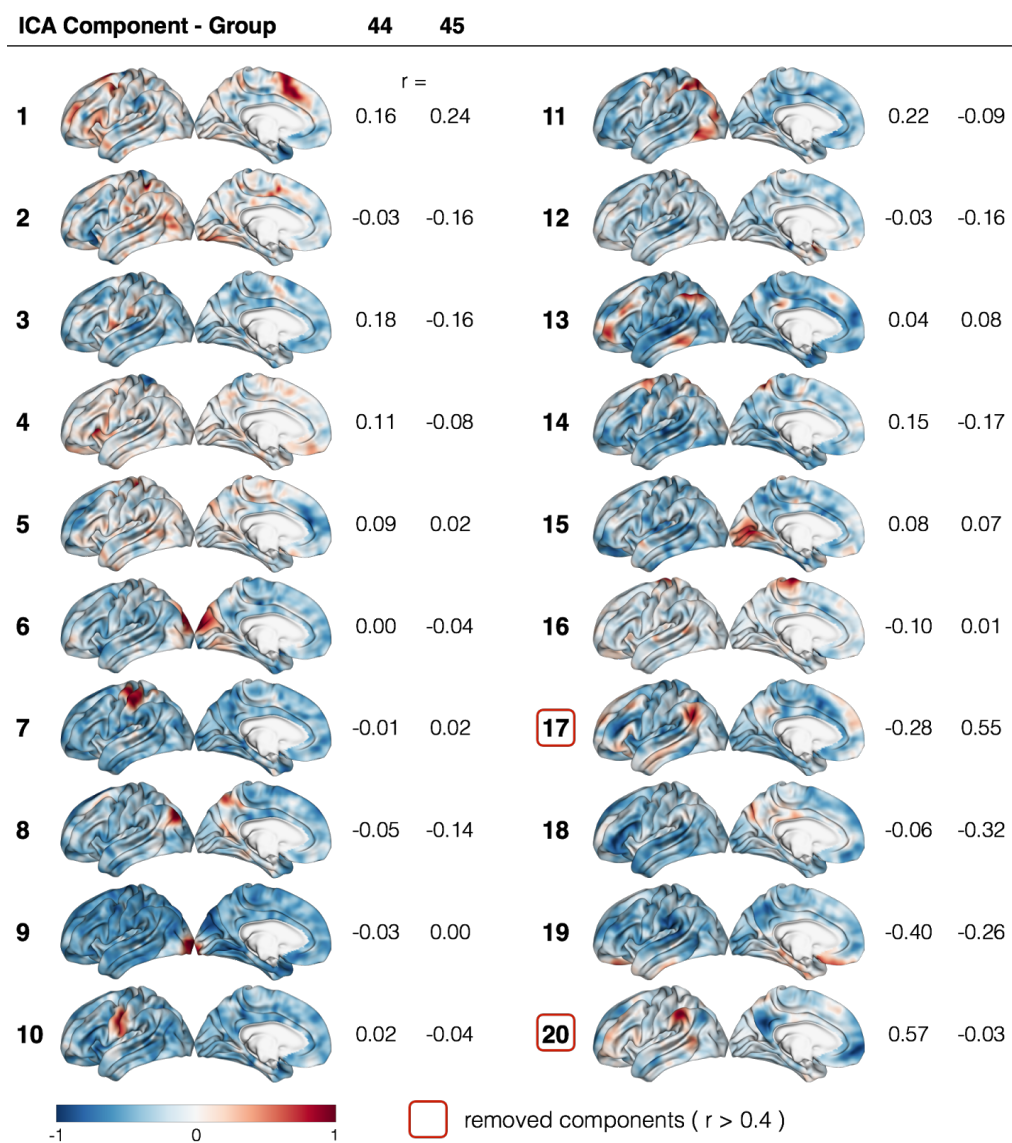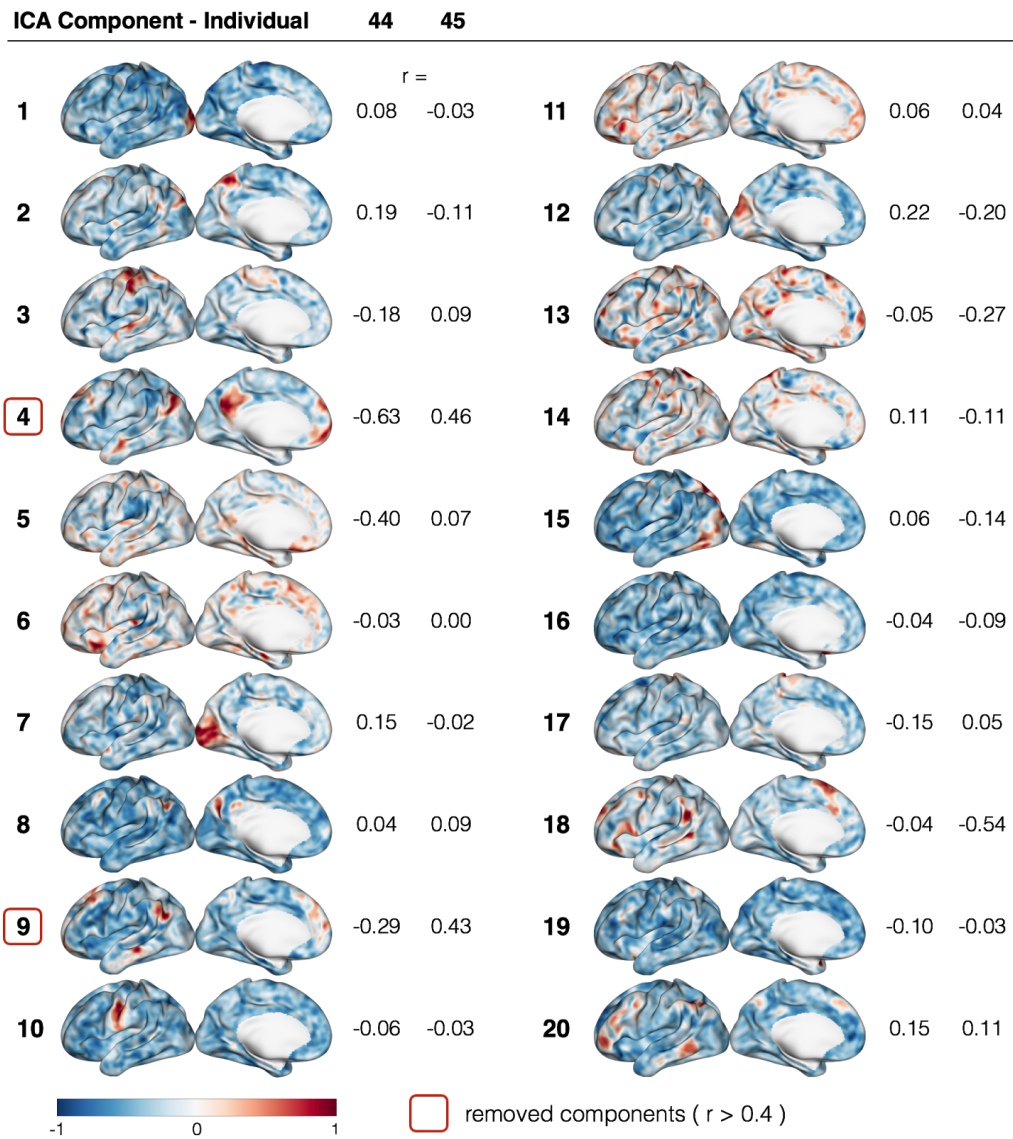
Figure 3.3: Results from the 20-component individual-level ICA of one HCP subject. Component maps with the highest spatial correlation with the individual-level seed-based connectivity templates of areas 44 and 45 were removed (outlined in red), and the remaining component maps were used in subsequent steps of the automated parcellation pipeline.
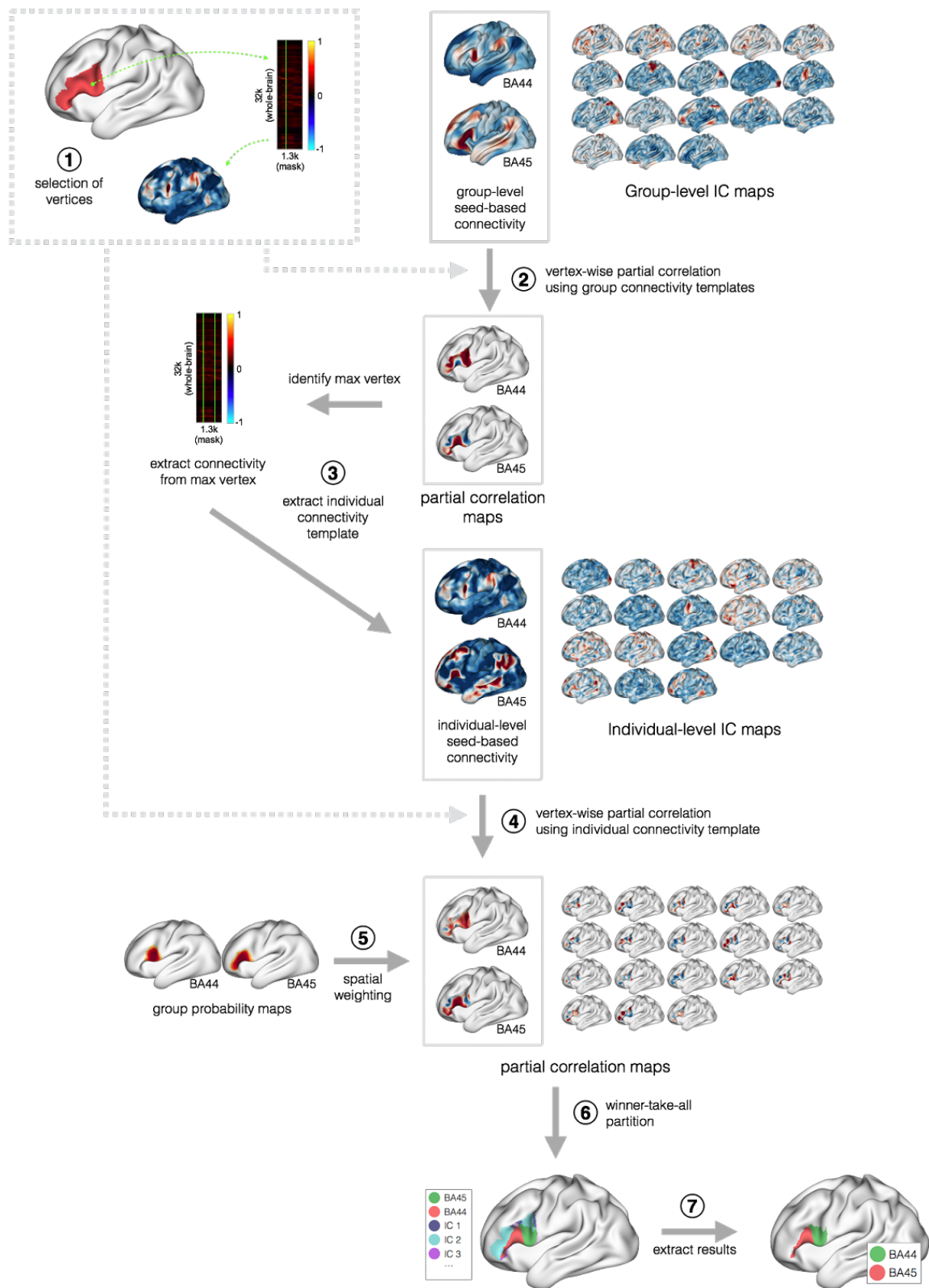
Figure 3.4: Pipeline for automated labeling of areas 44 and 45 in an individual subject. The labeling procedure consists of the following steps: (1) The whole-brain connectivity matrix of each individual subject is masked to a predefined ROI covering the ventrolateral prefrontal cortex. The following steps are then conducted on the whole-

brain connectivity map of each vertex within the ROI. (2) Vertex-wise partial correlations are run for areas 44 and 45 using group-level connectivity templates. (3) The vertices corresponding to the maximum partial correlation for areas 44 and 45 are identified, and used as seeds to extract individual-level connectivity templates. (4) Vertex-wise partial correlations are run using the individual-level seed-based connectivity templates of areas 44 and 45 and individual-level IC components. (5) A spatial weighting is applied to the partial correlation results for areas 44 and 45 using previously generated group-level spatial probability maps from manual labeling. (6) A winner-take-all partition is run across all resulting partial correlation maps. (7) The largest clusters corresponding to areas 44 and 45 are extracted.

3.2.4 Comparison of manual and automated parcellation results

To compare results from the manual and automated labeling procedures, the 101 previously manually labeled HCP datasets were run through the automated labeling pipeline. Spatial overlap of the area 44 and 45 labels from the manual and automated parcellation procedures were then compared using the Dice coefficient (DC) (Figure 3.5). The Dice coefficient (Dice, 1945) ranges between 0 and 1 and is defined as:

$$\frac{2|A \cap B|}{|A| + |B|}$$

To evaluate the effect of the spatial weighting applied in step 5 of the parcellation pipeline (Figure 3.4), the entire pipeline was repeated skipping this step.

3.2.5 Group-level comparisons

Group-level probability maps of areas 44 and 45 based on the results of the manual and automated parcellation procedures were then computed (Figure 3.6).

To obtain a label-specific measure of sulcal morphometry, we used the FreeSurfer *sulc* measure. This measure represents the displacement of a particular vertex on the cortical surface from a hypothetical surface in the midpoint between gyri and sulci, with a mean displacement of zero. The mean *sulc* value across the individual area 44 and 45 labels produced by manual and automated labeling was computed, and their distributions across subjects were compared.

3.2.6 Testing on an independent dataset

To confirm that the labeling pipeline can be applied to independent datasets with varying data acquisition and preprocessing parameters, the automated labeling procedure was applied to the 100 NKI datasets. Prior to labeling, the group-level connectivity and probability maps of areas 44 and 45 created using the manually labeled HCP datasets were downsampled from fs_LR_32k to fsaverage5 surface space. 20-component group- and individual-level independent component analyses were then run on the time series of the 100 NKI datasets.

To account for the lower quality of the NKI as compared to HCP data as well as the fact that the group-level connectivity templates of areas 44 and 45 were not derived from the same dataset, the threshold for removal of IC components was decreased to a correlation value of greater than 0.1. This resulted in more components being identified as related to BA 44 or 45 prior to running the partial correlation steps and subsequently regressing out fewer components, allowing for a higher degree of variability in the connectivity patterns within labels. All other aspects of the parcellation pipeline remained the same as for the HCP data. Group-level probability maps were then computed across the 100 NKI datasets for comparison (Figure 3.8). Eight of the 100 subjects were then manually labeled post hoc, blind to the results of the automated labeling, and spatial overlap of the automated and manual area 44 and 45 labels was compared using the Dice coefficient (Figure 3.9).

3.3 Results

3.3.1 Exclusion of one subject from automated parcellation

Of the 101 manually labeled HCP datasets, one subject was excluded from automated parcellation due to missing files in more recent HCP data releases. Removal of this subject has no effect on the results of the remaining subjects. The results of the automated parcellation are therefore presented for 100 of the 101 HCP subjects.

3.3.2 Comparison of manual and automated parcellation results

The results from the automated parcellation pipeline displayed a high degree of spatial overlap with the gold standard maps produced by manual labeling (Figure 3.5). The average Dice coefficient across the 100 subjects was 0.71 for area 45 and 0.63 for area 44. To demonstrate the improvement of the parcellation results when anatomical information is incorporated via spatial weighting of the partial correlation maps, results are additionally presented without the application of spatial weighting. For these results, the average Dice coefficient across the 100 subjects was 0.62 for area 45 and 0.39 for area 44 (note the markedly lower spatial overlap of the area 44 labels without spatial weighting).
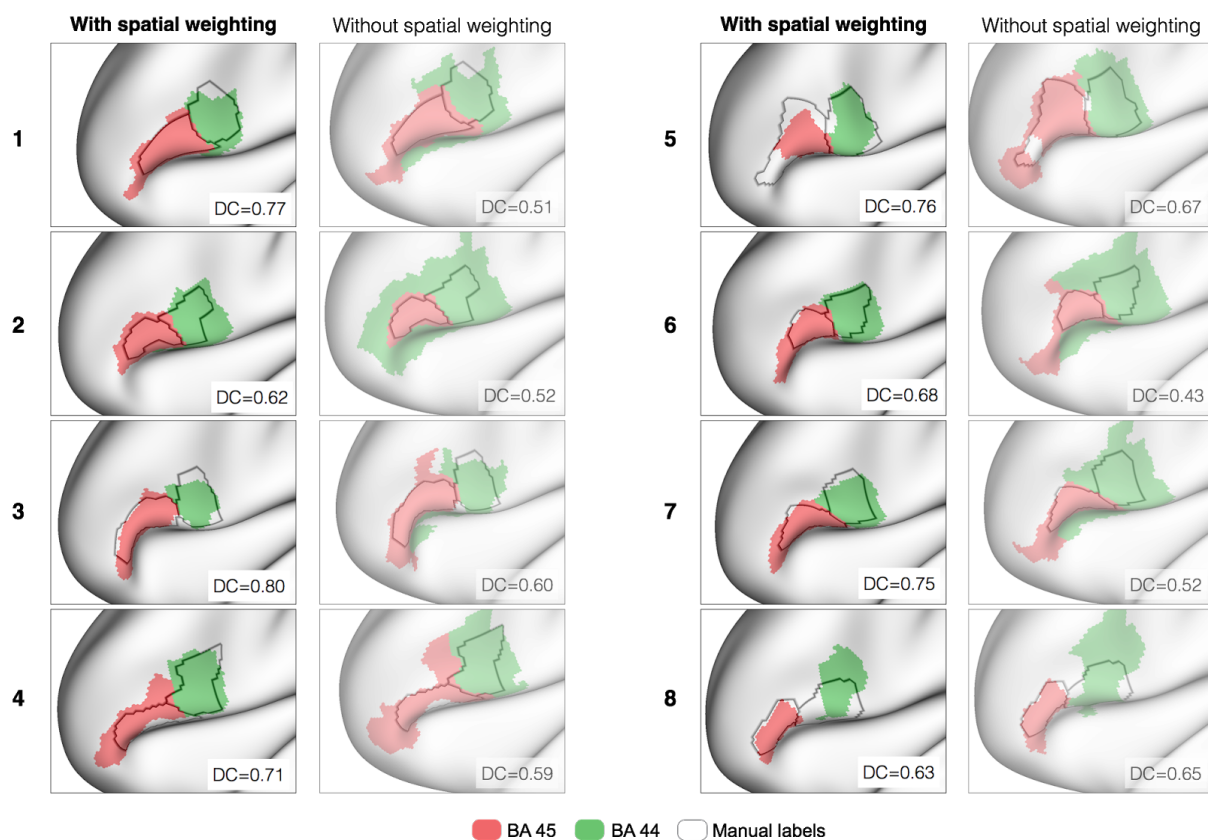
Figure 3.5: Spatial overlap of the manual (black contours) and automated (red and green) labels of areas 44 (green) and 45 (red) for eight of the 100 individual HCP subjects, with (left) and without (right) spatial weighting Dice coefficients have been averaged across areas 44 and 45 for each individual.

3.3.3 Group-level comparisons

The group-level probability maps of the labeled areas 44 and 45 demonstrate high consistency between the manual and automated labeling techniques. The region of highest overlap between subjects for area 45 is on the posterior half of the pars triangularis, directly anterior to the anterior ascending ramus of the lateral fissure. For area 44, the region of highest overlap lies on the anterior bank and fundus of the inferior precentral sulcus, adjacent to and including the pars opercularis. The functional connectivity-based group-level probability maps also show consistency with cytoarchitectonic probability maps derived from post-mortem histology (Amunts et al. 1999; Figure 3.6).
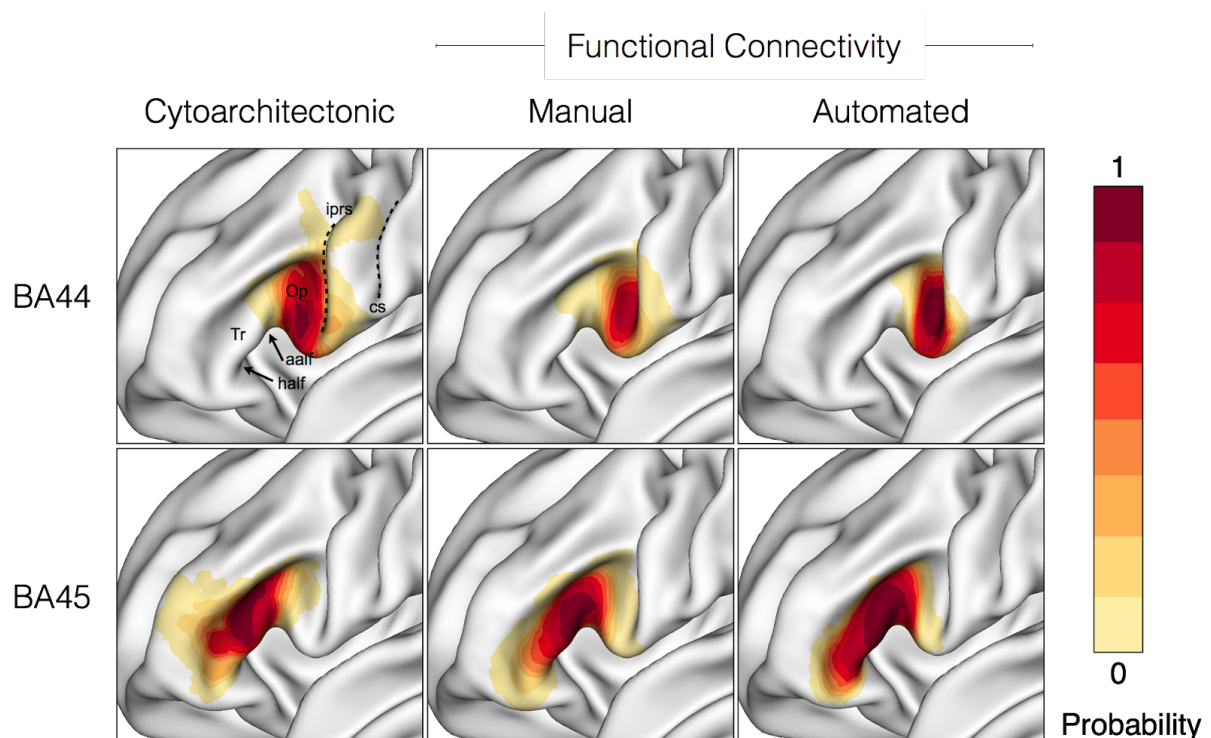
Figure 3.6: Group-average probability maps of areas 44 and 45 on the HCP fs_LR 32k 440-subject average surface, using different parcellation methods. From left: Probability maps from the Juelich Brain Model, based on cytoarchitectonic parcellation of 10 postmortem brains; Group-average masks from the manual parcellation of 100 functional connectivity datasets; Group-average masks from the automated parcellation of the same 100 functional connectivity datasets as used for manual parcellation. Abbreviations: aalf anterior ascending ramus of the lateral fissure; cs, central sulcus; half, horizontal anterior ramus of the lateral fissure; iprs, inferior precentral sulcus; Op, pars opercularis; Tr, pars triangularis.

Figure 3.7 shows the distribution of mean *sulc* value across the individual area 44 and 45 labels produced by manual and automated labeling for the 100 subjects. In the HCP data, sulci are represented by negative *sulc* values, and gyri by positive *sulc* values (note that this deviates from standard FreeSurfer convention). For both the manual and automated labeling, the mean *sulc* value for area 45 is consistently positive, suggesting that the area 45 labels include mostly gyral vertices. The mean *sulc* value across individuals for area 44 shows a wider distribution centered around zero for both the manual and automated labeling. This result is consistent with a higher degree of sulcal variability surrounding the pars opercularis as compared to the pars triangularis (Jakobsen et al. 2016), with the individual labels often extending into the inferior precentral sulcus. For both areas 44 and 45, the distributions of mean *sulc* values are wider for labels resulting from manual as compared to automated labeling, suggesting that the spatial weighting applied in the automated labeling pipeline is slightly more restrictive than in the manual labeling. However, a paired sample t-test revealed that the mean *sulc* values from the manual and automated labels are not significantly different (p=0.78 for area 45 and p=0.38 for area 44). For both manual and automated labeling, the mean *sulc* values from areas 44 and 45 were significantly different at p<0.001.
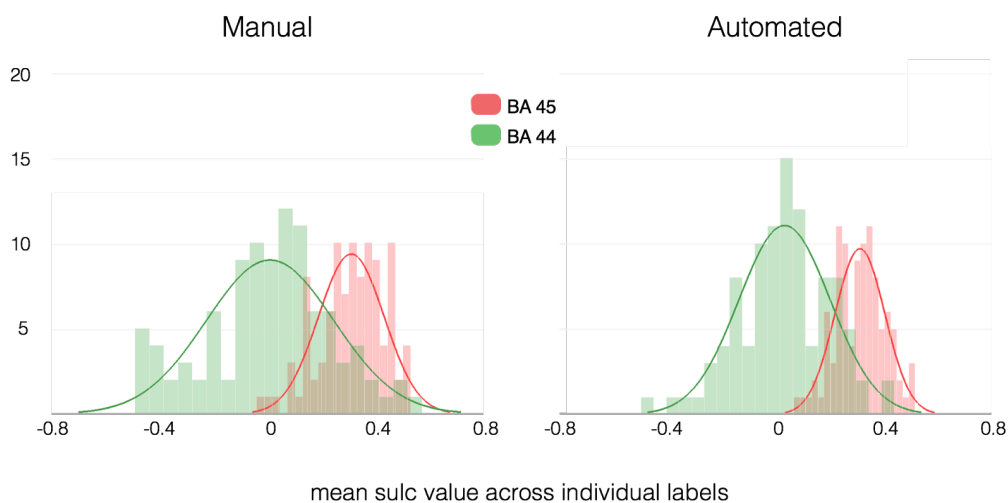
Figure 3.7: Distribution of mean FreeSurfer 'sulc' value across the individual area 44 and 45 labels produced by manual (left) and automated (right) labeling for the 100 original subjects. Sulci are represented by negative 'sulc' values, and gyri by positive 'sulc' values. Mean 'sulc' values from manual and automated labeling are not significantly different for area 45 (p=0.78) or area 44 (p=0.38).

3.3.4 Testing on an independent dataset

Figure 3.8 shows the group-level probability maps from automated labeling of the 100 NKI datasets. These maps are consistent with those from the HCP data as well as cytoarchitectonic probability maps derived from post-mortem histology (Figure 3.6).
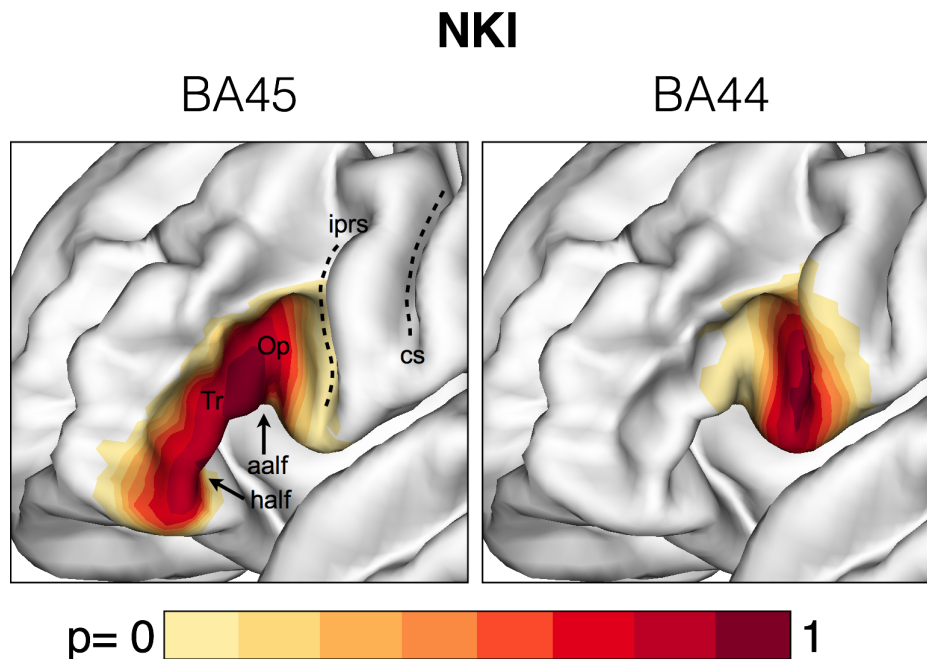
Figure 3.8: Group-average probability maps of areas 44 and 45 from automated labeling of the 100 NKI datasets, shown on the fsaverage5 surface.

The results of post hoc manual labeling on eight NKI datasets showed a high degree of spatial overlap with the area 44 and 45 labels produced by the automated labeling pipeline (Figure 3.9). The average Dice coefficient across the eight subjects was 0.71 for area 44 and 0.69 for area 45. These results demonstrate the ability of the automated labeling pipeline to generalize to datasets with varying resolution and acquisition parameters.
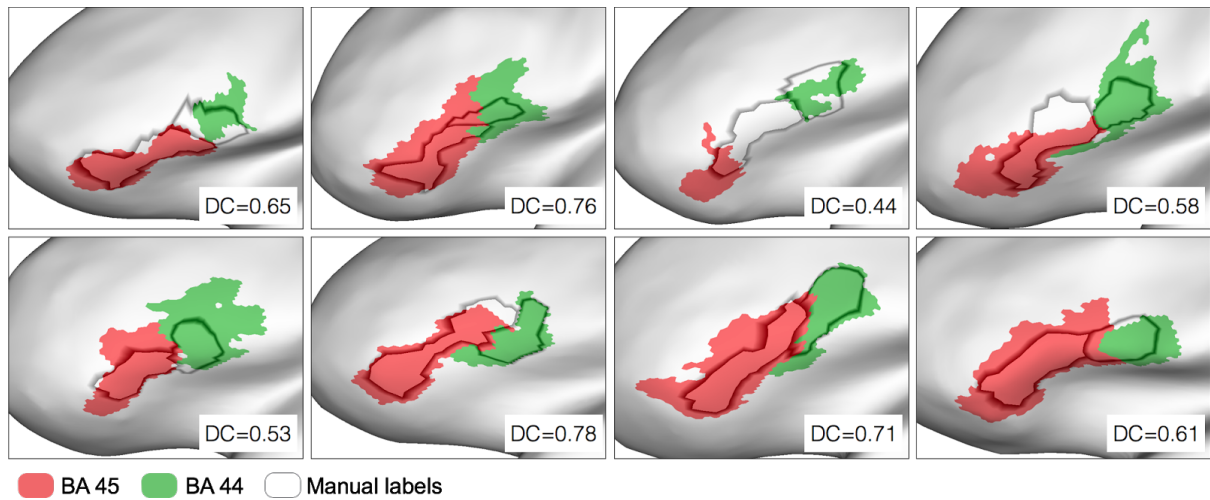
Figure 3.9: Spatial overlap of the manual (black contours) and automated (red and green) parcellation techniques for the eight NKI datasets for which post hoc manual labeling was performed, shown on the individual surfaces in fsaverage5 space. Dice coefficients have been averaged across areas 44 and 45 for each individual.

All results including individual subject labels and group-level probability maps are available for download online[5], as well as the automated labeling pipeline script[6].

3.4 Discussion

The results of the current study suggest that the automated parcellation pipeline is able to produce functional connectivity-based labels of areas 44 and 45 with comparable precision to the manual labeling procedure described in the previous chapter. The accuracy of parcellating and assigning labels in new datasets suggests that the method is not dependent on the specific cohort used to create the group-level connectivity templates and can be applied to independent functional connectivity datasets with varying scanning parameters.

Due to the high dimensionality and inherent complexity of functional connectivity data derived from resting-state fMRI, the development of data-driven parcellation techniques for dimensionality reduction has become a priority in the field (Thirion et al. 2014). Such approaches

---

[5] wwwuser.gwdg.de/~cbsarchi/archiv/public/hcp/

[6] github.com/NeuroanatomyAndConnectivity/broca/tree/master/PartialCorrelation

often make use of clustering algorithms, such as k-means, hierarchical, or spectral clustering, to group voxels or vertices into networks based on the similarity of their connectivity patterns (Yeo and Krienen et al. 2011; Kahnt et al. 2012; Craddock et al. 2012; Blumensath et al. 2013). Other methods make use of boundary detection techniques to map the transitions in connectivity patterns between cortical regions (Cohen et al., 2008; Hirose et al., 2012; Wig et al. 2014a). More recently, a method by Wang and colleagues (2015) made use of an iterative approach to fit a population-based functional atlas to individual brains, which critically and effectively captures cross-subject variability. These approaches for cortical parcellation are powerful tools for dimensionality reduction of complex functional connectivity data and can provide whole-brain functional atlases that are instrumental within particular research contexts.

The parcellation approach presented here differs from existing data-driven parcellation techniques by aiming to simulate the process of individual-level manual labeling driven by prior knowledge of the anatomy and connectivity of specific cortical areas. By targeting specific known differences in connectivity patterns and incorporating anatomical information via spatial weighting, the resulting area labels represent the best fit to the individual anatomy and connectivity. The two-step partial correlation approach using both group-level and individual template connectivity maps also ensures that cross-subject variance in connectivity patterns is accounted for. The availability of the manually labeled dataset is uniquely valuable for validation of the area labels derived from the automated parcellation pipeline, the accuracy of which would otherwise be difficult to quantify due to the lack of gold standard functional atlases.

The current study applied the automated parcellation pipeline to Broca's region where (i) the two cytoarchitectonic areas that comprise it are known to have distinct functional connectivity and (ii) the availability of the manually labeled datasets could provide a basis for comparison. However, the described parcellation pipeline could be modified to delineate any cortical regions for which known differences in functional connectivity exist and group-level connectivity

templates are available. In this case, the spatial probability maps based on the manually labeled datasets used for spatial weighting could be replaced with a different form of spatial information such as cytoarchitectonic probability maps or geodesic distance from an anatomically-defined ROI.

Like most cortical parcellation techniques, the current method provides deterministic binary labels of areas 44 and 45. However, it has recently been demonstrated that different cortical areas display varying degrees of sharpness in their boundaries (Wig et al. 2014a). For certain research applications it may therefore be advantageous to output probabilistic area labels at the individual level, and the parcellation criteria upon which the current method is based could just as well be used for this purpose. More specifically, the parcellation pipeline is very easily modified to output the partial correlation maps themselves, which, with the application of spatial weighting based on anatomical criteria, could serve as individual-level probabilistic area labels to be used for the investigation of transition gradients and quantification of the sharpness of boundaries across individuals.

Until recently, non-invasive *in vivo* definition of areas 44 and 45 has been a significant challenge and many functional neuroimaging studies have relied on anatomical definitions of the regions based on data derived from cytoarchitectonic studies. To our knowledge, no behavioral task exists that is able to reliably distinguish areas 44 and 45 from each other, and resting-state functional connectivity-based parcellation provides a solution to this problem. Our observer-independent parcellation method is able to produce probability maps based on both functional connectivity and anatomical location, which represent variability across a much larger number of individual brains than what is viable using invasive techniques. Additionally, we believe that the individual labels will prove useful for a variety of applications ranging from serving as functionally defined ROIs for fMRI studies to clinical applications such as presurgical planning.

This method fills a gap in the tools currently available for mapping the functional boundaries of specific cortical areas on an individual-level.

Chapter 4 - General discussion and outlook

4.1 Advantages and key contributions

The work presented in the current thesis aimed to make use of prior knowledge of the anatomical locations and connectivity differences within Broca's region to delineate the extent and boundaries of areas 44 and 45 in individual brains. The main advantages to this approach to cortical parcellation are:

1. It is non-invasive

2. It produces reliable functional labels at the individual level

3. It is multimodal, combining knowledge of both anatomy and connectivity

4. It can be applied to datasets with varying scanning and preprocessing parameters

The key contributions of this work are:

1. Proof-of-concept for the use of a novel functional connectivity visualization technique for individual-level manual delineation of cortical regions based on functional connectivity and morphological information.

2. Providing anatomy-informed group-level functional atlases as well as individual-level gold standard manual labels of areas 44 and 45 for a large number of individuals.

3. A novel tool for automated and observer-independent individual-level cortical parcellation of areas 44 and 45 informed by both functional connectivity and anatomy, and accounting for cross-subject variability.

4.2 Applications

All results and methods used in the present thesis have been made openly available in order to facilitate reproducibility and encourage further investigation. The parcellation techniques presented as well as the resulting area labels themselves have a variety of potential applications within both research and clinical contexts, which will be described briefly in the following sections.

4.2.1 Research applications

The individual-level labels as well as the group-level probability maps of areas 44 and 45 may prove useful for a variety of research applications. For example, the labels could be used as initialization for seed-based connectivity studies aiming to investigate sub-divisions of broader language networks, or as regions-of-interest for task-based fMRI studies in which accurate functional localization of areas 44 and 45 is essential to obtain reliable results due to their known functional specializations within language processing.

In more general terms, prior-informed functional atlases such as those presented here for areas 44 and 45 have a number of important research applications. One such application is to provide a framework for validating the results of other data-driven parcellation methods in the context of existing ontologies of brain function, which is an ongoing challenge in the field of brain parcellation. The current thesis demonstrated an example of such an application by making use of the manual labels to validate the results of the observer-independent automated parcellation technique by evaluating their spatial overlap in the same subjects. Without the availability of the manual labels, it would be difficult to determine whether or not the results of the automated labeling produced meaningful results. Similarly, the individual area labels or group-level atlases could be used to assign functional meaning to individual clusters identified using whole-brain

parcellation methods. This could subsequently aid in determining the appropriate number of clusters to assign, by choosing the results that best fit with existing functional atlases.

Functional atlases are also likely to prove useful in the development of new and improved strategies for the alignment of brain images. fMRI preprocessing commonly involves the registration of individual subjects' brains to a common template based on anatomical landmarks or features identified by structural MRI images (Fischl et al. 1999). Attempts have been made to improve this process by incorporating functional characteristics into the registration algorithms, for example by aligning regions based on functional similarity or connectivity (e.g. Sabuncu et al. 2010; Robinson et al. 2014). With this in mind, studies focused on investigating specific functions, such as language processing, may well benefit from registration algorithms tailored to align individual brains according to specific functional networks, such as those associated with Broca's region.

4.2.2 Clinical applications

Besides the many research applications outlined in the previous section, the ability to produce individual-level functional labels of areas involved in language processing has strong implications for clinical practice, especially in regards to presurgical planning. Neurosurgical procedures, such as operations to remove brain tumors, require accurate preoperative mapping in order to spare undamaged brain regions and thereby preserve cognitive function. Currently, non-invasive methods for presurgical mapping rely on task-based fMRI acquired under clinical conditions. Such data often suffers from poor signal-to-noise ratio (Parrish et al. 2000), and has been shown to have only limited correspondence with maps acquired through invasive techniques like direct cortical stimulation (Giussani et al. 2010). In contrast to task-based fMRI, resting-state fMRI acquisition is undemanding and therefore suitable for use with patients of all kinds. Additionally, while activations in parts of Broca's region are known to occur in numerous different behavioral tasks, no specific task paradigm has been identified that is able to reliably distinguish areas 44

and 45 from each other. Accurate and non-invasive functional mapping of areas 44 and 45 in individual patients based on resting-state data would therefore be particularly advantageous for patients requiring surgery within or near the ventrolateral frontal cortex.

As an alternative to additionally acquiring resting-state data from patients, which is not part of standard clinical protocol, the manual and automated parcellation methods could potentially be applied to bandpass-filtered task-fMRI data such as that acquired by default in a clinical context. Although this has not been tested for the methods presented in the current thesis, other similar cortical parcellation techniques based on functional connectivity have shown consistency in their results using resting-state versus band-pass filtered task-based fMRI (e.g. Wang et al. 2015). Although validation would of course be necessary, it is likely that the same would hold true for the parcellation methods presented here since the underlying data is essentially the same.

While the methods presented in the current thesis are certainly of interest within a clinical context, it remains to be determined whether they would perform reliably in clinical populations that may have undergone functional and structural reorganization due to brain injury or disease. For example, patients with localized lesions or tumors may present with distorted cortical anatomy and/or notable differences in functional connectivity patterns. This would present a challenge for the current implementation of the automated parcellation pipeline, which relies on some degree of cross-subject similarity as a starting point for individualized parcellations. Manual parcellation may therefore be more appropriate for clinical use since it is driven by the expertise of the user and can therefore more easily account for specific differences in individual patients. Regardless, validation and adaptation of the current version of either the manual or automated parcellation methods would be necessary to realize any potential clinical applications.

4.3 Outlook and future directions

4.3.1 Individual differences in cortical morphology

Studies on cortical morphology have shown that the ventrolateral frontal cortex exhibits particularly high interindividual variability (Keller et al., 2007), the most extreme cases of which result in some individual lacking certain sulci within this region entirely (Ono et al., 1990; Tomaiuolo et al., 1999). With this in mind, one intuitive application of the provided area labels is to further study the relationship between the extent and location of the individual functional labels to morphological features. Also relevant to this topic is the question of how these individual differences in both the morphology of these regions relate to behavioral traits and measures of language function. With the availability of a large amount of behavioral data from the same subjects as used in the present thesis via the Human Connectome Project, pursuing this future research direction is entirely feasible.

4.3.2 Lateralization of language function

The analyses presented in the current thesis only included the left cerebral hemisphere due to the strong left-lateralization of language function in approximately 96–98% of individuals (Rasmussen & Milner, 1975). However, most of what is known about the lateralization of language function is derived from invasive cortical stimulation procedures, which can only be performed on patients undergoing surgery due to brain lesions. Such patients may have experienced some degree of functional reorganization, which may in turn lead to a bias in the results towards a pathological state. A recent study using a non-invasive imaging technique measuring cerebral blood flow in healthy individuals found that 7.5% of right-handed participants presented with right-hemisphere dominance of language function, which is considerably higher than previously expected (Knecht et al. 2000). Additionally, the feasibility of using fluctuations in intrinsic brain activity to study lateralization of functional networks has been demonstrated in a study that used resting-state fMRI to map the most strongly lateralized

brain regions associated with various functional domains, including language (Liu et al. 2009). Based on these findings, it would be interesting to investigate in detail to what degree this strong left-lateralization of language networks is reflected in the functional connectivity associated with Broca's region and its right-hemisphere homologue. Both the manual and automated connectivity-based parcellation procedures presented here are just as easily applicable to the left and right hemispheres. Producing labels of areas 44 and 45 in both hemispheres in individual subjects would allow for the quantification of cross-hemispheric symmetry in the the extent and locations of these areas and thereby provide an alternative non-invasive measure of lateralization.

4.3.3 Transitions in connectivity and sharpness of boundaries

It has been shown that different cortical regions vary in the sharpness of their boundaries, with some areas displaying abrupt changes in connectivity and others transitioning gradually over a wider distance (Wig et al., 2014b). Additionally, there may be individual variability in the sharpness of specific area boundaries, as can be observed in the boundary between areas 44 and 45 using the manual labeling method. In order to study this variability, many new methods for detecting gradients or transitions in connectivity have recently been developed (Cohen et al., 2008; Hirose et al., 2009, 2012). Since gradient maps themselves do not contain information about the nature or location of the changes underlying the detected boundaries, combining these boundary detection approaches with parcellation methods informed by specific anatomical and connectivity features would provide a basis for characterizing the nature of specific boundaries between cortical areas.

4.3.4 Extension to other cortical regions

The current thesis presents methods for manual and automated cortical parcellation and applies them to the subdivision of Broca's region into its constituent areas 44 and 45. Broca's region is a natural candidate for prior-informed cortical parcellation due to its historical significance and the

large amount of knowledge that exists about its anatomy and connectivity. Additionally, the well-established role of Broca's region in language processing makes it and its subregions of particularly high relevance and interest to the fields of neuropsychology and cognitive neuroscience. That being said, the parcellation methods presented in the current thesis can be adapted to segment other cortical regions with the only criteria for successful application being the presence of distinct connectivity profiles and approximate anatomical landmarks associated with the areas. Although the automated parcellation pipeline requires the unique connectivity profiles of the areas to be known and used as templates for comparing the patterns of individual vertices, the manual parcellation technique could be used as a tool for interactive exploratory analysis of the connectivity patterns of less well-studied cortical regions. Manual parcellation could then be performed based on the user's observations of homogeneity within and differences between the connectivity patterns of anatomically-defined regions, and group-level connectivity templates could subsequently be created from the resulting manual labels and used as the basis for automated parcellation. Such work could help pave the way for the development of a whole-brain anatomy-informed functional parcellation technique.

References

Amunts, K., Lenzen, M., Friederici, A. D., Schleicher, A., Morosan, P., Palomero-Gallagher, N., et al. (2010). Broca's region: novel organizational principles and multiple receptor mapping. *PLoS Biology*, 8(9), e1000489.

Amunts, K., Schleicher, A., Bürgel, U., Mohlberg, H., Uylings, H., & Zilles, K. (1999). Broca's region revisited: cytoarchitecture and intersubject variability. *Journal of Comparative Neurology*, 412(2), 319-341.

Amunts, K., Schleicher, A., & Zilles, K. (2004). Outstanding language competence and cytoarchitecture in Broca's speech region. *Brain and Language*, 89(2), 346-353.

Amunts, K., & Zilles, K. (2015). Architectonic Mapping of the Human Brain Beyond Brodmann. *Neuron*, 88(6), 1086-1107.

Anwander, A., Tittgemeyer, M., von Cramon, D. Y., Friederici, A. D., & Knösche, T. R. (2007). Connectivity-based parcellation of Broca's area. *Cerebral Cortex*, 17(4), 816-825.

Arthur, D., & Vassilvitskii, S. (2007). k-means++: The advantages of careful seeding. *Proceedings of the Eighteenth Annual ACM-SIAM Symposium on Discrete Algorithms*. Society for Industrial and Applied Mathematics.

Bellec, P., Perlbarg, V., Jbabdi, S., Pélégrini-Issac, M., Anton, J., Doyon, J., et al. (2006). Identification of large-scale networks in the brain using fMRI. *NeuroImage*, 29(4), 1231-1243.

Bellec, P., Lavoie-Courchesne, S., Dickinson, P., Lerch, J., Zijdenbos, A., & Evans, A. C. (2012). The pipeline system for Octave and Matlab (PSOM): a lightweight scripting framework and execution engine for scientific workflows. *Frontiers in Neuroinformatics*, 6, 7.

Bilz, F. E. (1894). *Das neue Heilverfahren: Lehrbuch d. naturgemäßen Heilweise u. Gesundheitspflege*. Bilz, Dresden.

Birn, R. M., Molloy, E. K., Patriat, R., Parker, T., Meier, T. B., Kirk, G. R., et al. (2013). The effect of scan length on the reliability of resting-state fMRI connectivity estimates. *NeuroImage*, 83, 550-558.

Biswal, B., Zerrin Yetkin, F., Haughton, V. M., & Hyde, J. S. (1995). Functional connectivity in the motor cortex of resting human brain using echo-planar mri. *Magnetic Resonance in Medicine*, 34(4), 537-541.

Blumensath, T., Jbabdi, S., Glasser, M. F., Van Essen, D. C., Ugurbil, K., Behrens, T. E., et al. (2013). Spatially constrained hierarchical parcellation of the brain with resting-state fMRI. *NeuroImage*, 76, 313-324.

Brodmann, K. (1909). *Vergleichende Lokalisationslehre der Grosshirnrinde in ihren Prinzipien dargestellt auf Grund des Zellenbaues*. Barth, Leipzig.

Broca, P. (1861a). Perte de la parole, ramollissement chronique et destruction partielle du lobe antérieur gauche du cerveau. *Bulletin de la Societe d'Anthropologie*, 2(1), 235-238.

Broca, P. (1861b). Remarques sur le siège de la faculté du langage articulé, suivies d'une observation d'aphémie (perte de la parole). *Bulletins de la Société d'anatomie (Paris)*, 2e serie 1861c, 6, 330-57.

Broca, P. (1861c). Nouvelle observation d'aphemie produite par une lesion de la troisieme circonvolution frontale. *Bulletins de la Societe d'anatomie (Paris)*, 398-407.

Böttger, J., Schurade, R., Jakobsen, E., Schaefer, A., & Margulies, D. S. (2014). Connexel visualization: a software implementation of glyphs and edge-bundling for dense connectivity data using brainGL. *Frontiers in Neuroscience*, 8, 15.

Catani, M. & Jones, D.K. (2005) Perisylvian language networks of the human brain. *Annals of Neurology*, 57, 8–16.

Clos, M., Amunts, K., Laird, A. R., Fox, P. T., & Eickhoff, S. B. (2013). Tackling the multifunctional nature of Broca's region meta-analytically: co-activation-based parcellation of area 44. *NeuroImage*, 83, 174-188.

Cohen, A. L., Fair, D. A., Dosenbach, N. U., Miezin, F. M., Dierker, D., Van Essen, D. C., et al. (2008). Defining functional areas in individual human brains using resting functional connectivity MRI. *NeuroImage*, 41(1), 45-57.

Craddock, R. C., James, G. A., Holtzheimer, P. E., Hu, X. P., & Mayberg, H. S. (2012). A whole brain fMRI atlas generated via spatially constrained spectral clustering. *Human Brain Mapping*, 33(8), 1914-1928.

Damoiseaux, J. S., & Greicius, M. D. (2009). Greater than the sum of its parts: a review of studies combining structural connectivity and resting-state functional connectivity. *Brain Structure and Function*, 213(6), 525-533.

Desikan, R. S., Ségonne, F., Fischl, B., Quinn, B. T., Dickerson, B. C., Blacker, D., et al. (2006). An automated labeling system for subdividing the human cerebral cortex on MRI scans into gyral based regions of interest. *NeuroImage*, 31(3), 968-980.

Dice, L. R. (1945). Measures of the amount of ecologic association between species. *Ecology*, 26(3), 297-302.

Dronkers, N. F., Plaisant, O., Iba-Zizen, M. T., & Cabanis, E. A. (2007). Paul Broca's historic cases: high resolution MR imaging of the brains of Leborgne and Lelong. *Brain*, 130(5), 1432-1441.

Fischl, B., Sereno, M. I., & Dale, A. M. (1999). Cortical surface-based analysis: II: inflation, flattening, and a surface-based coordinate system. *NeuroImage*, 9(2), 195-207.

Fischl, B., Salat, D. H., Busa, E., Albert, M., Dieterich, M., Haselgrove, C., et al. (2002). Whole brain segmentation: automated labeling of neuroanatomical structures in the human brain. *Neuron*, 33(3), 341-355.

Fisher, R. A. (1915). Frequency distribution of the values of the correlation coefficient in samples from an indefinitely large population. *Biometrika*, 10(4), 507-521.

Fisher, R. A. (1921). On the 'probable error' of a coefficient of correlation deduced from a small sample. *Metron,* 1, 3–32.

Fox, M. D., & Raichle, M. E. (2007). Spontaneous fluctuations in brain activity observed with functional magnetic resonance imaging. *Nature Reviews Neuroscience*, 8(9), 700-711.

Frey, S., Campbell, J. S., Pike, G. B., & Petrides, M. (2008). Dissociating the human language pathways with high angular resolution diffusion fiber tractography. *The Journal of Neuroscience*, 28(45), 11435-11444.

Frey, S., Mackey, S., & Petrides, M. (2014). Cortico-cortical connections of areas 44 and 45B in the macaque monkey. *Brain and Language*, 131, 36-55.

Gall, F. J., & Spurzheim, G. (1818). *Anatomie et physiologie du systême nerveux en général, et du cerveau en particulier: avec des observations sur la possibilité de reconnoitre plusieurs dispositions intellectuelles et morales de l'homme et des animaux par la configuration de leurs têtes (Vol. 3).* F. Schoell.

Gao, W., Elton, A., Zhu, H., Alcauter, S., Smith, J. K., Gilmore, J. H., et al. (2014). Intersubject variability of and genetic effects on the brain's functional connectivity during infancy. *The Journal of Neuroscience*, 34(34), 11288-11296.

Gerbella, M., Belmalih, A., Borra, E., Rozzi, S., & Luppino, G. (2010). Cortical connections of the macaque caudal ventrolateral prefrontal areas 45A and 45B. *Cerebral Cortex*, 20(1), 141-168.

Goder, A., & Filkov, V. (2008). Consensus clustering algorithms: Comparison and refinement. Proceedings of the Meeting on Algorithm Engineering & Experiments. *Society for Industrial and Applied Mathematics.*

Giussani, C., Roux, F., Ojemann, J., Sganzerla, E. P., Pirillo, D., & Papagno, C. (2010). Is preoperative functional magnetic resonance imaging reliable for language areas mapping in brain tumor surgery? Review of language functional magnetic resonance imaging and direct cortical stimulation correlation studies. *Neurosurgery*, 66(1), 113-120.

Heim, S., Alter, K., Ischebeck, A. K., Amunts, K., Eickhoff, S. B., Mohlberg, H., et al. (2005). The role of the left Brodmann's areas 44 and 45 in reading words and pseudowords. *Cognitive Brain Research*, 25(3), 982-993.

Hirose, S., Chikazoe, J., Jimura, K., Yamashita, K., Miyashita, Y., & Konishi, S. (2009). Sub-centimeter scale functional organization in human inferior frontal gyrus. *NeuroImage*, 47(2), 442-450.

Hirose, S., Watanabe, T., Jimura, K., Katsura, M., Kunimatsu, A., Abe, O., et al. (2012). Local signal time-series during rest used for areal boundary mapping in individual human brains. *PloS ONE*, 7(5), e36496.

Honey, C., Sporns, O., Cammoun, L., Gigandet, X., Thiran, J., Meuli, R., et al. (2009). Predicting human resting-state functional connectivity from structural connectivity. *Proceedings of the National Academy of Sciences*, 106(6), 2035-2040.

Hutchison, R. M., & Everling, S. (2012). Monkey in the middle: Why non-human primates are needed to bridge the gap in resting-state investigations. *Frontiers in Neuroanatomy*, 6, 29.

Hutchison, R. M., Womelsdorf, T., Gati, J. S., Everling, S., & Menon, R. S. (2013). Resting−state networks show dynamic functional connectivity in awake humans and anesthetized macaques. *Human Brain Mapping*, 34(9), 2154-2177.

Jakobsen, E., Boettger, J., Bellec, P., Geyer, S., Ruebsamen, R., Petrides, M., Margulies, D.S. (2016). Subdivision of Broca's region based on individual−level functional connectivity. *European Journal of Neuroscience*, 43(4), 561-571.

Kahnt, T., Chang, L. J., Park, S. Q., Heinzle, J., & Haynes, J. (2012). Connectivity-based parcellation of the human orbitofrontal cortex. *The Journal of Neuroscience*, 32(18), 6240-6250.

Katzev, M., Tüscher, O., Hennig, J., Weiller, C., & Kaller, C. P. (2013). Revisiting the functional specialization of left inferior frontal gyrus in phonological and semantic fluency: the crucial role of task demands and individual ability. *The Journal of Neuroscience*, 33(18), 7837-7845.

Keller, S. S., Highley, J. R., Garcia−Finana, M., Sluming, V., Rezaie, R., & Roberts, N. (2007). Sulcal variability, stereological measurement and asymmetry of Broca's area on MR images. *Journal of Anatomy*, 211(4), 534-555.

Kelly, C., Uddin, L. Q., Shehzad, Z., Margulies, D. S., Castellanos, F. X., Milham, M. P., et al. (2010). Broca's region: linking human brain functional connectivity data and non−human primate tracing anatomy studies. *European Journal of Neuroscience*, 32(3), 383-398.

Klein, J. C., Behrens, T. E., Robson, M. D., Mackay, C. E., Higham, D. J., & Johansen-Berg, H. (2007). Connectivity-based parcellation of human cortex using diffusion MRI: establishing reproducibility, validity and observer independence in BA 44/45 and SMA/pre-SMA. *NeuroImage*, 34(1), 204-211.

Knecht, S., Deppe, M., Dräger, B., Bobe, L., Lohmann, H., Ringelstein, E., et al. (2000). Language lateralization in healthy right-handers. *Brain*, 123(1), 74-81.

Krings, T., Erberich, S. G., Roessler, F., Reul, J., & Thron, A. (1999). MR blood oxygenation level–dependent signal differences in parenchymal and large draining vessels: implications for functional MR imaging. *American Journal of Neuroradiology*, 20(10), 1907-1914.

Le Bihan, D., Breton, E., Lallemand, D., Grenier, P., Cabanis, E., & Laval-Jeantet, M. (1986). MR imaging of intravoxel incoherent motions: application to diffusion and perfusion in neurologic disorders. *Radiology*, 161(2), 401-407.

Liu, H., Stufflebeam, S. M., Sepulcre, J., Hedden, T., & Buckner, R. L. (2009). Evidence from intrinsic activity that asymmetry of the human brain is controlled by multiple factors. *Proceedings of the National Academy of Sciences*, 106(48), 20499-20503.

Margulies, D. S., Böttger, J., Watanabe, A., & Gorgolewski, K. J. (2013). Visualizing the human connectome. *NeuroImage*, 80, 445-461.

Margulies, D. S., & Petrides, M. (2013). Distinct parietal and temporal connectivity profiles of ventrolateral frontal areas involved in language production. *The Journal of Neuroscience*, 33(42), 16846-16852.

Margulies, D. S., Vincent, J. L., Kelly, C., Lohmann, G., Uddin, L. Q., Biswal, B. B., et al. (2009). Precuneus shares intrinsic functional architecture in humans and monkeys. *Proceedings of the National Academy of Sciences*, 106(47), 20069-20074.

Mars, R. B., Jbabdi, S., Sallet, J., O'Reilly, J. X., Croxson, P. L., Olivier, E., et al. (2011). Diffusion-weighted imaging tractography-based parcellation of the human parietal cortex and comparison with human and macaque resting-state functional connectivity. *The Journal of Neuroscience*, 31(11), 4087-4100.

Mesulam, M. (1990). Large-scale neurocognitive networks and distributed processing for attention, language, and memory. *Annals of Neurology*, 28(5), 597-613.

Miranda-Dominguez, O., Mills, B. D., Grayson, D., Woodall, A., Grant, K. A., Kroenke, C. D., et al. (2014). Bridging the gap between the human and macaque connectome: a quantitative comparison of global interspecies structure-function relationships and network topology. *The Journal of Neuroscience*, 34(16), 5552-5563.

Mueller, S., Wang, D., Fox, M. D., Yeo, B. T., Sepulcre, J., Sabuncu, M. R., et al. (2013). Individual variability in functional connectivity architecture of the human brain. *Neuron*, 77(3), 586-595.

Murtagh, F. & Legendre, P. (2011) Ward's hierarchical clustering method: clustering criterion and agglomerative algorithm. *arXiv preprint*, arXiv:1111.6285.

Neubert, F., Mars, R. B., Thomas, A. G., Sallet, J., & Rushworth, M. F. (2014). Comparison of human ventral frontal cortex areas for cognitive control and language with areas in monkey frontal cortex. *Neuron*, 81(3), 700-713.

Nock, R., & Nielsen, F. (2006). On weighting clustering. Pattern Analysis and Machine Intelligence. *IEEE Transactions on*, 28(8), 1223-1235.

Nooner, K., Colcombe, S., Tobe, R., Mennes, M., Benedict, M., Moreno, A., et al. (2012). The NKI-Rockland sample: a model for accelerating the pace of discovery science in psychiatry. *Frontiers in Neuroscience*, 6, 152.

Ogawa, S., Lee, T., Kay, A. R., & Tank, D. W. (1990). Brain magnetic resonance imaging with contrast dependent on blood oxygenation. *Proceedings of the National Academy of Sciences*, 87(24), 9868-9872.

Ojemann, J. G., Akbudak, E., Snyder, A. Z., McKinstry, R. C., Raichle, M. E., & Conturo, T. E. (1997). Anatomic localization and quantitative analysis of gradient refocused echo-planar fMRI susceptibility artifacts. *NeuroImage*, 6(3), 156-167.

Ojemann, G., Ojemann, J., Lettich, E., & Berger, M. (1989). Cortical language localization in left, dominant hemisphere: an electrical stimulation mapping investigation in 117 patients. *Journal of Neurosurgery*, 71(3), 316-326.

Ono, M., Kubik, S., & Abernathey, C. D. (1990). *Atlas of the Cerebral Sulci*. Thieme Medical Publishers, New York.

Parrish, T. B., Gitelman, D. R., LaBar, K. S., & Mesulam, M. (2000). Impact of signal-to-noise on functional MRI. *Magnetic Resonance in Medicine*, 44(6), 925-932.

Penfield, W., & Roberts, L. (1959). *Speech and brain mechanisms*. Princeton University Press, Princeton.

Petrides, M., Alivisatos, B., & EvANs, A. C. (1995). Functional activation of the human ventrolateral frontal cortex during mnemonic retrieval of verbal information. *Proceedings of the National Academy of Sciences*, 92(13), 5803-5807.

Petrides, M., & Pandya, D. (1994) Comparative architectonic analysis of the human and the macaque frontal cortex, in: F. Boller, J. Grafman (Eds.), *Handbook of Neuropsychology*, 9, Elsevier, Amsterdam (1994), pp. 17–58

Petrides, M., & Pandya, D. (1999). Dorsolateral prefrontal cortex: comparative cytoarchitectonic analysis in the human and the macaque brain and corticocortical connection patterns. *European Journal of Neuroscience*, 11(3), 1011-1036.

Petrides, M., & Pandya, D. (2002). Comparative cytoarchitectonic analysis of the human and the macaque ventrolateral prefrontal cortex and corticocortical connection patterns in the monkey. *European Journal of Neuroscience*, 16(2), 291-310.

Petrides, M., & Pandya, D. N. (2009). Distinct parietal and temporal pathways to the homologues of Broca's area in the monkey. *PLoS Biology*, 7(8), e1000170.

Petrides, M. (2013). *Neuroanatomy of Language Regions of the Human Brain*. Academic Press.

Poldrack, R. A., Wagner, A. D., Prull, M. W., Desmond, J. E., Glover, G. H., & Gabrieli, J. D. (1999). Functional specialization for semantic and phonological processing in the left inferior prefrontal cortex. *NeuroImage*, 10(1), 15-35.

Rasmussen, T., & Milner, B. (1975). Clinical and surgical studies of the cerebral speech areas in man. *Cerebral Localization*, 238-257.

Robinson, E. C., Jbabdi, S., Glasser, M. F., Andersson, J., Burgess, G. C., Harms, M. P., et al. (2014). MSM: A new flexible framework for Multimodal Surface Matching. *NeuroImage*, 100, 414-426.

Sabuncu, M. R., Singer, B. D., Conroy, B., Bryan, R. E., Ramadge, P. J., & Haxby, J. V. (2010). Function-based intersubject alignment of human cortical anatomy. *Cerebral Cortex*, 20(1), 130-140.

Sahin, N. T., Pinker, S., Cash, S. S., Schomer, D., & Halgren, E. (2009). Sequential processing of lexical, grammatical, and phonological information within Broca's area. *Science*, 326(5951), 445-449.

Salimi-Khorshidi, G., Douaud, G., Beckmann, C. F., Glasser, M. F., Griffanti, L., & Smith, S. M. (2014). Automatic denoising of functional MRI data: combining independent component analysis and hierarchical fusion of classifiers. *NeuroImage*, 90, 449-468.

Sallet, J., Mars, R. B., Noonan, M. P., Neubert, F., Jbabdi, S., O'Reilly, J. X., et al. (2013). The organization of dorsal frontal cortex in humans and macaques. *The Journal of Neuroscience*, 33(30), 12255-12274.

Sepulcre, J., Liu, H., Talukdar, T., Martincorena, I., Yeo, B. T., & Buckner, R. L. (2010). The organization of local and distant functional connectivity in the human brain. *PLoS Computational Biology*, 6(6), e1000808.

Smith, S. M., Beckmann, C. F., Andersson, J., Auerbach, E. J., Bijsterbosch, J., Douaud, G., et al. (2013). Resting-state fMRI in the human connectome project. *NeuroImage*, 80, 144-168.

Tate, M. C., Herbet, G., Moritz-Gasser, S., Tate, J. E., & Duffau, H. (2014). Probabilistic map of critical functional regions of the human cerebral cortex: Broca's area revisited. *Brain*, 137(10), 2773-2782.

Thirion, B., Varoquaux, G., Dohmatob, E., & Poline, J. (2014). Which fMRI clustering gives good brain parcellations?. *Frontiers in Neuroscience*, 8(167), 13.

Tomaiuolo, F., MacDonald, J., Caramanos, Z., Posner, G., Chiavaras, M., Evans, A. C., et al. (1999). Morphology, morphometry and probability mapping of the pars opercularis of the inferior frontal gyrus: an in vivo MRI analysis. *European Journal of Neuroscience*, 11(9), 3033-3046.

Van Den Heuvel, M. P., & Pol, H. E. H. (2010). Exploring the brain network: a review on resting-state fMRI functional connectivity. *European Neuropsychopharmacology*, 20(8), 519-534.

Van Dijk, K. R., Hedden, T., Venkataraman, A., Evans, K. C., Lazar, S. W., & Buckner, R. L. (2010). Intrinsic functional connectivity as a tool for human connectomics: theory, properties, and optimization. *Journal of Neurophysiology*, 103(1), 297-321.

Vincent, J., Patel, G., Fox, M., Snyder, A., Baker, J., Van Essen, D., et al. (2007). Intrinsic functional architecture in the anaesthetized monkey brain. *Nature*, 447(7140), 83-86.

Wang, D., Buckner, R. L., Fox, M. D., Holt, D. J., Holmes, A. J., Stoecklein, S., et al. (2015). Parcellating cortical functional networks in individuals. *Nature Neuroscience*, 18, 1853–1860.

Wig, G. S., Laumann, T. O., Cohen, A. L., Power, J. D., Nelson, S. M., Glasser, M. F., et al. (2014a). Parcellating an individual subject's cortical and subcortical brain structures using snowball sampling of resting-state correlations. *Cerebral Cortex*, 24(8), 2036-2054.

Wig, G. S., Laumann, T. O., & Petersen, S. E. (2014b). An approach for parcellating human cortical areas using resting-state correlations. *NeuroImage*, 93, 276-291.

Yeo, B. T., Krienen, F. M., Sepulcre, J., Sabuncu, M. R., Lashkari, D., Hollinshead, M., et al. (2011). The organization of the human cerebral cortex estimated by intrinsic functional connectivity. *Journal of Neurophysiology*, 106(3), 1125-1165.

Yoon, U., Lee, J., Kim, J., Lee, S. M., Kim, I. Y., Kwon, J. S., et al. (2003). Modified magnetic resonance image based parcellation method for cerebral cortex using successive fuzzy clustering and boundary detection. *Annals of Biomedical Engineering*, 31(4), 441-447.

Summary

Introduction

The notion that the cerebral cortex can be subdivided into distinct subregions with specific structural and functional features is one of the fundamental guiding principles of human cognitive neuroscience. This idea can be partly attributed to the historically significant discovery of Broca's region, a part of the inferior frontal cortex known to play a significant role in speech production and language processing. Broca's region is comprised of two adjacent cytoarchitectonic areas, 44 and 45, which are commonly defined based on specific macroanatomical landmarks of the inferior frontal gyrus.

Early invasive cortical stimulation studies in humans provided the first evidence of functional differentiation between areas 44 and 45. While modern functional magnetic resonance imaging (fMRI) studies have also suggested a functional specialization of areas 44 and 45, there is some discrepancy regarding the precise range of functions that can be attributed to these two areas since no behavioral task exists that is able to reliably distinguish them. It is generally agreed that area 44 is mainly involved in speech production while area 45 is more involved in higher-level semantic aspects of language processing such as verbal fluency. Nevertheless, the inherent difficulty in accurately defining even the most well-studied brain regions such as areas 44 and 45 using task-based fMRI represents a clear need for the development of new methods for *in vivo* cortical parcellation.

Based on both invasive tract-tracing and non-invasive diffusion imaging tractography studies, it has been established that areas 44 and 45 and their homologues have distinct structural connectivity to superior temporal and inferior parietal regions in both macaque monkeys and

humans. Recent studies have shown that these structural connectivity differences are mirrored in functional connectivity estimated by resting-state fMRI, which measures intrinsic fluctuations in brain activity in the absence of stimuli. In the context of these findings, resting-state functional connectivity combined with knowledge of the approximate anatomical locations of areas 44 and 45 provides a solid basis from which to develop prior-informed methods for reliable parcellation of these two areas in individual brains *in vivo*.

The work described in the the present thesis is comprised of two main projects, the overarching goal of which is to make use of prior knowledge of the anatomical locations and functional connectivity differences within Broca's region to delineate the extent and boundaries of areas 44 and 45 in individual brains. The first project describes a novel technique for the manual parcellation of the two areas based on differences in functional connectivity and anatomical priors. The second project builds on the results of the first project by using the manual labels in the development an automated and observer-independent methods for cortical parcellation that aims to mimic and have comparable precision to the manual parcellation approach at the individual level.

Project 1

Project 1 presents the first application of a novel functional connectivity visualization technique for the manual parcellation of cortical areas in individual brains. This technique makes use of prior knowledge of functional connectivity in conjunction with morphological information to manually delineate the extent and boundaries of cortical areas in individual brains. Results are presented from the application of the technique to the subdivision of Broca's region into its constituent areas 44 and 45 in a large number of individual brains.

For this project, 101 resting-state functional magnetic resonance imaging datasets from the Human Connectome Project were used. Left-hemisphere surface-based correlation matrices

were computed and visualized in an in-house software package called brainGL, developed especially for this purpose. By observation of differences in the connectivity patterns of neighbouring points on the cortical surface, areas 44 and 45 were manually parcellated in individual brains, and then compared at the group-level. Additionally, the manual labelling approach was compared with parcellation results based on several pre-existing data-driven parcellation algorithms such as k-means and hierarchical clustering. Areas 44 and 45 could be clearly distinguished from each other in all individuals, and the manual segmentation method showed high test-retest reliability. Group-level probability maps of areas 44 and 45 showed spatial consistency across individuals, and corresponded well to cytoarchitectonic probability maps based on *post mortem* data. Group-level connectivity maps were also consistent with previous studies showing distinct connectivity patterns of areas 44 and 45.

The key contributions of Project 1 are: (1) providing a reliable method for individual-level cortical parcellation that could be applied to regions distinguishable by even the most subtle differences in patterns of functional connectivity, and (2) providing anatomy-informed group-level functional atlases as well as individual-level gold standard manual labels of areas 44 and 45 for a large number of individuals.

Project 2

Project 2 builds on the results of Project 1 by developing an automated and data-driven cortical parcellation technique that mimics the manual labeling approach to produce area labels with comparable precision at the individual level. While the manual parcellation method provides a reliable way to define cortical regions, it is also highly labor- and time-intensive and relies heavily on the expertise of the user. For this reason, the development of an observer-independent alternative technique is an important step in the overall research agenda. The automated parcellation technique is again applied to the sub-parcellation of Broca's region into its

constituent areas 44 and 45 in a large number of individual brains, and the results of the manual and automated labeling approaches are compared at the individual level.

The method first extracts individualized connectivity templates of areas 44 and 45 by assigning to each surface vertex within the ventrolateral frontal cortex the partial correlation value of its functional connectivity to group-level templates of areas 44 and 45, accounting for other template connectivity patterns. To account for cross-subject variability in connectivity, the partial correlation procedure is then repeated using individual-level network templates, including individual-level connectivity from areas 44 and 45. Each node is finally labeled as area 44, 45, or neither, using a winner-take-all approach. The method also incorporates prior knowledge of anatomical location by weighting the results using spatial probability maps obtained from manual labeling. The resulting area labels show a high degree of spatial overlap with the gold-standard manual labels, and group-average area maps are consistent with cytoarchitectonic probability maps of areas 44 and 45. To facilitate reproducibility and to demonstrate that the method can be applied to resting-state fMRI datasets with varying acquisition and preprocessing parameters, the labeling procedure is applied to two independent open-source datasets from the Human Connectome Project and the Nathan Kline Institute Rockland Sample. While this project focuses on sub-dividing Broca's region, the method is adaptable to parcellate other cortical regions with distinct connectivity profiles.

The key contribution of project 2 is the presentation of a novel tool for automated and observer-independent individual-level cortical parcellation of areas 44 and 45 informed by both functional connectivity and anatomy, and accounting for cross-subject variability.

Conclusions

To date, cytoarchitectonic probability maps derived from invasive *post mortem* studies have been considered the gold standard for defining cortical areas. The methods presented in the current

thesis provide a non-invasive alternative method for parcellating cortical areas *in vivo* at both the individual and group levels. This approach differs from existing methods for parcellating cortical areas based on functional connectivity in that it integrates prior knowledge of specific cortical regions by basing parcellations on a combination of area-specific anatomical and connectivity features. The parcellation techniques presented as well as the resulting area labels themselves have a variety of potential applications within both research and clinical contexts, which are discussed in detail in Chapter 4. Besides the current application to sub-dividing Broca's region, the methods could be adapted to any regions of the brain with distinct connectivity profiles, representing a valuable contribution to the current methods available for *in vivo* cortical parcellation.

Zusammenfassung

Einleitung

Es gehört zu den grundlegenden Prinzipien der kognitiven Neurowissenschaften, dass die menschliche Großhirnrinde (Kortex) in unterschiedliche Subregionen mit jeweils spezifischen strukturellen und funktionellen Eigenschaften unterteilt werden kann. Diese Erkenntnis kann zum Teil auf die historisch bedeutsame Entdeckung des Broca-Areals zurückgeführt werden, das als Teil des inferioren frontalen Kortex wichtig für die Sprachproduktion und -verarbeitung ist. Das Broca-Areal besteht aus zwei benachbarten, zytoarchitektonischen Feldern, 44 und 45, die gemeinhin durch spezifische makroanatomische Landmarken des inferioren frontalen Gyrus lokalisiert werden.

Frühe, invasive Stimulationsstudien am Menschen erbrachten erste Belege für eine funktionelle Differenzierung der Felder 44 and 45. Auch aktuelle funktionelle Magnetresonanztomografie (fMRT) Studien legen eine funktionelle Spezialisierung von Feld 44 und 45 nah. Dennoch is weiterhin unklar welche genauen Funktionen den jeweiligen Feldern zugeordnet werden können, da bisher keine Verhaltensaufgabe existiert, die zuverlässig zwischen den Feldern unterscheidet. Grundsätzlich besteht Einigkeit darüber, dass Feld 44 hauptsächlich in Sprachproduktion, Feld 45 hingegen eher in übergeordnete, semantische Aspekten der Sprachverarbeitung, z.B. Sprachfluss, involviert ist. Nichtsdestotrotz weist die grundsätzliche Schwierigkeit sogar einige der meistuntersuchtesten Gehirnregionen wie Feld 44 and 45 mittels verhaltensbasiertem fMRT exakt zu definieren, auf eine eindeutige Notwendigkeit zur Entwicklung neuer Methoden der kortikalen Parzellierung in vivo hin.

Mithilfe invasiver Traktographie und nicht-invasiver Diffusionstrakographie konnte gezeigt werden, dass die Felder 44 und 45 unterschiedliche strukurelle Konnektivität zu superior temporalen and inferior parietalen Regionen aufweisen, sowohl in Menschen also auch in homologen Regionen in Makaken. Neuere Studien haben darüber hinaus gezeigt, dass sich diese Unterschiede in der strukturellen Konnektivität auch in der funktionellen Konnektivität widerspiegeln. Funktionelle Konnektivität wird hierbei durch Kohärenz intrinsischer Fluktuationen der Gehirnaktivität in Abwesenheit äußerer Reize in fMRT-Ruhezustandsmessungen gemessen. In Anbetracht dieser Befunde stellen fMRT-Ruhezustandsmessungen in Kombination mit dem bisherigen Wissen über die ungefähre anatomische Lage der Felder 44 und 45 eine solide Basis dar, von der aus a priori informierte Methoden zur reliablen in vivo Parzellierung der beiden Felder entwickelt werden können.

Die in der vorliegenden Arbeit beschriebene Studie besteht aus zwei Hauptprojekten, deren übergeordnetes Ziel die exakte Beschreibung der Ausmaße und Grenzen der Felder 44 und 45 in individuellen Gehirnen ist. Vorkenntnissen über die anatomische Lage sowie Unterschiede in der funktionellen Konnektivität innerhalb des Broca-Areals bilden hierfür die Grundlage. Das erste Projekt beschreibt eine neuartige Technik zur manuellen Parzellierung der beiden Felder, die auf funktionellen Konnektivitätsunterschieden und anatomischen Vorkenntnissen beruht. Das zweite Projekt baut auf den Resultaten des ersten Projekts auf. Hier wird die manuelle Parzellierung genutzt um eine automatisierte und beobachterunabhängige Methode zur kortikalen Parzellierung zu entwickeln, die im Ergebnis und in der Präzision mit dem manuellen Ansatz vergleichbar ist.

Projekt 1

Projekt 1 beinhaltet die erste Anwendung einer neuen Visualisierungstechnik funktioneller Konnektivität zur manuellen Parzellierung kortikaler Regionen in individuellen Gehirnen. Die Technik nutzt Vorwissen über funktionelle Konnektivtät in Kombination mit morphologischer

Information, um das Ausmaß und die Grenzen kortikaler Regionen in individuellen Gehirnen manuell zu ermessen. Diese Technik wurde zur Einteilung des Broca Areals in die Felder 44 und 45 in einer grossen Anzahl individueller Gehirne angewendet.

Für dieses Projekt wurden 101 Ruhezustands-fMRT-Datensätze des Human Connectome Projects verwendet. Korrelationsmatrizen für die Oberflächen der linken Hirnhälften wurden errechnet und mit einer eigens hierfür entwickelten Software, brainGL, visualisiert. Die Felder 44 und 45 wurden manuell aufgrund der Unterschiede in Konnektivitätsmustern benachbarter kortikaler Oberflächenpunkte auf individueller Ebene parzelliert und dann auf der Gruppenebene verglichen. Zudem wurden die Ergebnisse dieser manuellen Methode mit Parzellierungsresultaten verschiedener existierender datenbasierter Parzellationsalgorithmen wie "k-means" und "hierarchical clustering" verglichen. Die Felder 44 und 45 konnten in allen Individuen deutlich voneinander unterschieden werden und die manuelle Segmentierungsmethode zeigte die höchste test-retest Reliabilität. Gruppenbasierte Wahrscheinlichkeitskarten der Felder 44 und 45 wiesen gute interindividuelle räumliche Konsistenz auf und stimmten mit zytoarchitektonischen Warscheinlichkeitskarten von post mortem Daten überein. Gruppenbasierte Konnektivitätskarten waren ebenfalls konsistent mit vorherigen Studien, in denen verschiedene Konnektivitätsmuster für die Felder 44 und 45 gezeigt wurden.

Die Hauptbeiträge des ersten Projekts sind: (1) eine zuverlässige Methode zur kortikalen Parzellierung auf individueller Ebene, anwendbar auf Regionen, die sich durch selbst kleinste Unterschiede in funktionellen Konnektivitätsmustern voneinander unterschieden lassen, und (2) ein gruppenbasierter, anatomisch informierter, funktioneller Atlas der Felder 44 und 45, sowie nach manuellem Goldstandard gekennzeichnete Felder 44 und 45 auf individueller Ebene in einer großen Anzahl von Individuen.

Projekt 2

Projekt 2 basiert auf den Ergebnissen von Projekt 1: Es wurde eine automatisierte und datengeleitete kortikale Parzellierungstechnik entwickelt, die den manuellen Ansatz der Kennzeichnung imitiert und eine vergleichbare Präzision auf individueller Ebene erreicht. Die manuelle Parzellierung stellt eine zuverlässige Methode dar um kortikale Regionen zu definieren, die jedoch sehr zeit- und arbeitsintensiv ist und zudem stark von der Expertise des Anwenders abhängt. Aus diesem Grund ist die Entwicklung einer beobachterunabhängigen Methode eine wichtiger Schritt in der Forschungsagenda. Die automatisierte Parzellierungstechnik wurde erneut in einer großen Anzahl individueller Gehirne angewendet um das Broca-Areal in die Felder 44 und 45 zu unterteilen. Die Ergebnisse der manuellen und automatischen Markierungsansätze werden auf individueller Ebene verglichen.

Die vorgestellte Methode extrahiert in einem ersten Schritt individualisierte Konnektivitätsmuster für de Felder 44 und 45. Dafür wird jedem Oberflächenpunkt des ventrolateralen frontalen Kortex der partielle Korrelationswert seiner funktionellen Konnektivtät mit den Gruppenmustern der Felder 44 und 45 zugewiesen, wobei für andere Konnektivitätsmuster kontrolliert wird. Einem "winner-take-all" Ansatz folgend wird schließlich jeder Punkt dem Feld 44, 45, oder keinem der beiden zugeordnet. Diese Methode berücksichtigt ebenfalls anatomisches Vorwissen, indem sie die räumlichen Wahrscheinlichkeitskarten des manuellen Markierungsprozesses in die Gewichtung der Ergebinsse einbezieht. Die erlangten Feldmarkierungen zeigen ein hohes Mass an räumlicher Kohärenz mit dem Goldstandard der manuellen Markierung. Zudem stimmen die Gruppendurchschnittswerte der Regionenkarten mit den zytoarchitektonischen Wahrscheinlichkeitkarten der Felder 44 und 45 überein. Um die Reproduzierbarkeit zu vereinfachen und um zu zeigen, dass unsere Methode auf Ruhezustands-fMRT-Datensätze mit unterschiedlichen Erherbungs- und Vorverarbeitungsparametern angewendet werden kann, wird das Markierungsverfahren auf zwei unabhängige, öffentlich

verfügbare Datensätze angewendet, die aus dem Human Connectome Project beziehungsweise dem Nathan Kline Institute Rockland Sample stammen. Der Fokus liegt auf der Parzellierung des Broca-Areals, die Methode ist jedoch ebenfalls für die Parzellierungen anderer kortikaler Regionen mit charakteristischen Konnektivitätsprofilen anwendbar.

Der Hauptbeitrag des zweiten Projekts ist die Einführung einer neuen Methode zur automatisierten und beobachterunabhängigen Parzellierung der Felder 44 und 45 auf individueller Ebene. Die Methode nutzt Vorwissen über die funktionelle Konnektivität und anatomische Lage und trägt der interindividuellen Variabilität Rechnung.

Schlussfolgerungen

Derzeit werden zytoarchitektonische Wahrscheinlichkeitskarten aus invasiven post mortem Studien als Goldstandard für die Definition kortikaler Areale betrachtet. Die in dieser Arbeit präsentierten Methoden stellen eine nicht-invasive Alternative zur Parzellierung kortikaler Areale in vivo dar, sowohl auf individueller also auch auf Gruppenebene. Dieser Ansatz unterscheidet sich von existierenden Methoden der Parzellierung kortikaler Areale indem Vorwissen über Anatomie und Konnektivitätsprofil einzelner Regionen kombiniert und der Parzellierung zugrunde gelegt wird. Die vorgestellten Parzellierungstechniken sowie die resultierenden Kennzeichnungen der Areale können sowohl im Forschungsbereich als auch im klinischen Kontext vielseitig angewendet werden, wie in Kapitel 4 ausgeführt. Neben der hier beschriebenen Anwendung für die Unterteilung des Broca-Areals, können die Methoden auf jegliche Hirnregionen mit abgrenzbaren Konnektivitätsprofilen angewendet werden. Dies stellt einen wertvollen Beitrag zu den derzeit verfügbaren Methoden der kortikalen in vivo Parzellierung dar.

Curriculum Vitae

Estrid Nystrup Jakobsen
04. June 1989, Fredensborg, Denmark

EDUCATION

2012-present   Max Planck Institute for Human Cognitive and Brain Sciences
                University of Leipzig, Germany
                PhD Student, IMPRS NeuroCom

2010-2011   Institute of Psychiatry, King's College London, United Kingdom
                MSc Neuroscience (awarded with Distinction)

2007-2010   University of Westminster, United Kingdom
                BSc (Hons) Cognitive Science (awarded with First Class Honours)

2003-2007   American School of The Hague, The Netherlands
                International Baccalaureate Diploma

RESEARCH EXPERIENCE

02-04.2012   Research Assistant
                Department of Psychology, University of Westminster, London, UK
                Grant proposal preparation for research on cognitive rehabilitation in hydrocephalus patients

02-04.2010   Research Assistant
                Meath School (specialist speech and language primary school), Ottershaw, UK
                Development of a new tool for language skill level assessment in children with severe language impairment

08-09.2009   Laboratory Assistant
                Kennedy Krieger Institute, Johns Hopkins University, MD, USA
                Animal care, neurosurgery assistance, laboratory work including use of cryostat and sliding microtome, tissue staining, and microscopy

---

AWARDS AND SCHOLARSHIPS

2016   Erasmus Mundus Exchange Network in Auditory Cognitive Neuroscience Fellowship
2015   PhD graduation scholarship - FAZIT-Stiftung
2015   Travel Award to attend OHBM 2015 in Honolulu, Hawaii - Research Academy Leipzig
2014   Travel Award to attend OHBM 2014 in Hamburg, Germany - Research Academy Leipzig
2012   IMPRS NeuroCom Stipend - Max Planck Society
2010   Tuition bursary for academic achievement - King's College London
2008   Progression award for academic achievement - University of Westminster

Publications and conference contributions

PEER-REVIEWED PUBLICATIONS

Jakobsen, E., Margulies, D.S. Automated individual-level parcellation of Broca's region based on functional connectivity. *NeuroImage* (in press)

Kuehn, E.*, Dinse, J.*, **Jakobsen, E.**, Long, X., Schaefer, A., Bazin, PL., Sereno, M., Villringer, A., Margulies, D.S. Topographic parcellation of human sensory and motor cortex. *Cerebral Cortex* (in press)

Jakobsen, E., Böttger, J., Bellec, P., Geyer, S., Rübsamen, R., Petrides, M., Margulies, D.S. (2016) Subdivision of Broca's region based on individual-level functional connectivity. *European Journal of Neuroscience* 43(4).

Böttger, J., Schurade, R., **Jakobsen, E.**, Schäfer, A., & Margulies, D.S. (2014). Connexel visualization: A software implementation of glyphs and edge-bundling for dense connectivity data using brainGL. *Frontiers in Neuroscience* 8(15).

Catani, M., Mesulam, M. M., **Jakobsen, E.**, Malik, F., Matersteck, A., Wieneke, C., Thompson, C. K., Thiebaut de Schotten, M., Dell'Acqua, F., Weintraub, S., & Rogalski, E. (2013). A novel frontal pathway underlies verbal fluency in primary progressive aphasia. *Brain* 136(8).

TALKS/LECTURES

Jakobsen, E. (2015). *The Restless Brain.* Presented at: The Science and Politics of Laziness, Wellcome Collection, London, UK.

Jakobsen, E. (2015). *Individual in vivo sub-parcellation of Broca's region using functional connectivity glyphs.* Presented at the 43rd Annual Meeting of the International Neuropsychological Society, Denver, Colorado, USA.

Margulies, D.S., **Jakobsen, E.** (2015). *Visualizing Connectivity.* IMPRS NeuroCom advanced lectures on connectivity. Max Planck Institute for Human Cognitive and Brain Sciences, Leipzig, Germany.

POSTERS

Klados, M., Lauckner, M., **Jakobsen, E.**, Margulies, D.S. (2016). *Characterizing the Primary Spectrum of Personality and Brain Connectivity.* Presented at the 22nd Annual Meeting of the Organization for Human Brain Mapping (OHBM), Geneva, Switzerland.

Jakobsen, E., Klados, M., Zelmer, J., Goulas, A., & Margulies, D.S. (2014). *Automated sub-parcellation of Broca's region based on resting-state functional connectivity.* Presented at the 21st Annual Meeting of the Organization for Human Brain Mapping (OHBM), Honolulu, HI, USA.

Jakobsen, E., Chaze, C., Böttger, J., Geyer, S., Turner, R., Petrides, M., & Margulies, D.S. (2014). *Cortical parcellation of Broca's region based on functional connectivity glyphs*. Presented at 4th IMPRS NeuroCom Summer School, London, UK.

Jakobsen, E., Chaze, C., Böttger, J., Geyer, S., Turner, R., Petrides, M., & Margulies, D.S. (2014). *Cortical parcellation of Broca's region based on functional connectivity glyphs*. Presented at the 20th Annual Meeting of the Organization for Human Brain Mapping (OHBM), Hamburg, Germany.

D'Anna, L., Mesulam, M., Thiebaut de Schotten, M., **Jakobsen, E.**, Wieneke, C., Dell'Acqua, F., Rogalski, E., Catani, M. (2014). *Abnormalities of the uncinate fasciculus correlate with behavioural symptoms in primary progressive aphasia*. Presented at the 20th Annual Meeting of the Organization for Human Brain Mapping (OHBM), Hamburg, Germany.

Jakobsen, E., Boettger, J., Geyer, S., & Margulies, D. S. (2013). *Cortical parcellation of ventrolateral prefrontal cortex based on functional connectivity glyphs*. Presented at 3rd IMPRS NeuroCom Summer School, Leipzig, Germany.

Catani, M., Mesulam, M. M., **Jakobsen, E.**, Malik, F., Matersteck, A., Wieneke, C., Thompson, C. K., Thiebaut de Schotten, M., Dell'Acqua, F., Weintraub, S., & Rogalski, E. (2013). *A novel frontal pathway underlies verbal fluency in primary progressive aphasia*. Presented at the 19th Annual Meeting of the Organization for Human Brain Mapping (OHBM), Seattle, Washington, USA.

Statement of Authorship

This is to confirm that the work presented in this thesis has been performed and interpreted solely by myself, except where explicitly identified to the contrary. The contents of this thesis in full or in part, have not been submitted to any other institute or university for the fulfillment of any degree or diploma.

_____

Leipzig, 13.07.2016   Estrid Nystrup Jakobsen